CCSDS

The Consultative Committee for Space Data Systems

Report Concerning Space Data System Standards

BANDWIDTH-EFFICIENT MODULATIONS

SUMMARY OF DEFINITION, IMPLEMENTATION, AND PERFORMANCE

INFORMATIONAL REPORT

CCSDS 413.0-G-2

GREEN BOOK
October 2009

CCSDS

The Consultative Committee for Space Data Systems

Report Concerning Space Data System Standards

BANDWIDTH-EFFICIENT MODULATIONS

SUMMARY OF DEFINITION, IMPLEMENTATION, AND PERFORMANCE

INFORMATIONAL REPORT

CCSDS 413.0-G-2

GREEN BOOK

October 2009

AUTHORITY

Issue:	Informational Report, Issue 2
Date:	October 2009
Location:	Washington, DC, USA

This document has been approved for publication by the Management Council of the Consultative Committee for Space Data Systems (CCSDS) and reflects the consensus of technical panel experts from CCSDS Member Agencies. The procedure for review and authorization of CCSDS Reports is detailed in the *Procedures Manual for the Consultative Committee for Space Data Systems*.

This document is published and maintained by:

> CCSDS Secretariat
> Space Communications and Navigation Office, 7L70
> Space Operations Mission Directorate
> NASA Headquarters
> Washington, DC 20546-0001, USA

FOREWORD

This Report contains technical material to supplement the CCSDS recommendations for the standardization of modulation methods for high symbol rate transmissions generated by CCSDS Member Agencies.

Through the process of normal evolution, it is expected that expansion, deletion, or modification of this document may occur. This Report is therefore subject to CCSDS document management and change control procedures, which are defined in the *Procedures Manual for the Consultative Committee for Space Data Systems*. Current versions of CCSDS documents are maintained at the CCSDS Web site:

http://www.ccsds.org/

Questions relating to the contents or status of this document should be addressed to the CCSDS Secretariat at the address indicated on page i.

At time of publication, the active Member and Observer Agencies of the CCSDS were:

Member Agencies

- Agenzia Spaziale Italiana (ASI)/Italy.
- British National Space Centre (BNSC)/United Kingdom.
- Canadian Space Agency (CSA)/Canada.
- Centre National d'Etudes Spatiales (CNES)/France.
- China National Space Administration (CNSA)/People's Republic of China.
- Deutsches Zentrum für Luft- und Raumfahrt e.V. (DLR)/Germany.
- European Space Agency (ESA)/Europe.
- Russian Federal Space Agency (RFSA)/Russian Federation.
- Instituto Nacional de Pesquisas Espaciais (INPE)/Brazil.
- Japan Aerospace Exploration Agency (JAXA)/Japan.
- National Aeronautics and Space Administration (NASA)/USA.

Observer Agencies

- Austrian Space Agency (ASA)/Austria.
- Belgian Federal Science Policy Office (BFSPO)/Belgium.
- Central Research Institute of Machine Building (TsNIIMash)/Russian Federation.
- Centro Tecnico Aeroespacial (CTA)/Brazil.
- Chinese Academy of Sciences (CAS)/China.
- Chinese Academy of Space Technology (CAST)/China.
- Commonwealth Scientific and Industrial Research Organization (CSIRO)/Australia.
- CSIR Satellite Applications Centre (CSIR)/Republic of South Africa.
- Danish National Space Center (DNSC)/Denmark.
- European Organization for the Exploitation of Meteorological Satellites (EUMETSAT)/Europe.
- European Telecommunications Satellite Organization (EUTELSAT)/Europe.
- Geo-Informatics and Space Technology Development Agency (GISTDA)/Thailand.
- Hellenic National Space Committee (HNSC)/Greece.
- Indian Space Research Organization (ISRO)/India.
- Institute of Space Research (IKI)/Russian Federation.
- KFKI Research Institute for Particle & Nuclear Physics (KFKI)/Hungary.
- Korea Aerospace Research Institute (KARI)/Korea.
- Ministry of Communications (MOC)/Israel.
- National Institute of Information and Communications Technology (NICT)/Japan.
- National Oceanic and Atmospheric Administration (NOAA)/USA.
- National Space Organization (NSPO)/Chinese Taipei.
- Naval Center for Space Technology (NCST)/USA.
- Scientific and Technological Research Council of Turkey (TUBITAK)/Turkey.
- Space and Upper Atmosphere Research Commission (SUPARCO)/Pakistan.
- Swedish Space Corporation (SSC)/Sweden.
- United States Geological Survey (USGS)/USA.

DOCUMENT CONTROL

Document	Title	Date	Status
CCSDS 413.0-G-1	Bandwidth-Efficient Modulations: Summary of Definition, Implementation, and Performance, Issue 1	April 2003	Original issue, superseded
CCSDS 413.0-G-2	Bandwidth-Efficient Modulations: Summary of Definition, Implementation, and Performance, Informational Report, Issue 2	October 2009	Current issue

CONTENTS

CONTENTS (continued)

CONTENTS (continued)

1   INTRODUCTION

1.1   PURPOSE AND SCOPE

Since their inception, the various international space agencies have operated an ever-increasing number of science missions in the Earth Exploration Satellite Service (EESS) and Space Research Service (SRS) bands. The data transport requirements of these missions have also continued to escalate, with the result that the finite spectrum resources are now becoming increasingly strained.

To mitigate this situation and reduce the possibility of adjacent channel interference, spectrum advisory and regulatory agencies such as the Space Frequency Coordination Group (SFCG) and the International Telecommunication Union (ITU) have recently enacted out-of-band emission mask recommendations. These masks are designed to severely restrict the power in that portion of transmitted signal falling outside some necessary bandwidth.

CCSDS has responded by developing a series of recommendations for standard bandwidth-efficient modulation techniques applicable to high rate missions in selected SRS and EESS bands. These modulations were selected based on their spectral containment characteristics, with the characteristics of the SFCG Recommendation 17-2R1 mask[1] serving as a minimum requirement. Bit Error Rate (BER) performance, compatibility with existing infrastructure, and suitability for cross-support were also significant factors in selecting modulations for these recommendations.

This Green Book provides the background information for CCSDS recommendations 401(2.4.17A), 401(2.4.17B) and 401(2.4.18) addressing the use of spacecraft telemetry bandwidth-efficient modulations which were approved by the CCSDS Management Council in June 2001. This document provides a technical specification for the modulation techniques approved in the above-mentioned recommendations, together with a description of their main performance characteristics for the applications covered by the recommendations. All figures are simulations unless noted otherwise.

This document includes two annexes. Annex A is a glossary of acronyms used in the document. Annex B provides simulated performance data of the efficient modulations when amplified by a Solid State Power Amplifier (SSPA) operating with 0 dB output backoff referenced to maximum output power. This data includes occupied bandwidth, BER, and interference susceptibility of the bandwidth-efficient modulations. The data provided in annex B is indicative of system performance expected using the reference model. Performance of other systems will be highly dependent upon their transmitter and receiver characteristics. The performance data in annex B was extracted from study reports available in reference [1].

---

[1] Modified and renumbered in 2001 as SFCG Recommendation 21-2.

1.2 APPLICABILITY

The modulation techniques described in this document are applicable to high symbol rate (> 2 Ms/s for 2 and 8 GHz space research, and > 20 Ms/s for 32 GHz space research) telemetry transmissions for missions in the SRS and EESS. Three classes of modulation techniques are identified:

- Those dedicated to space research, Category A missions, specified in recommendation 401(2.4.17A) B-1. They are applicable to frequency bands 2200-2290 MHz and 8450-8500 MHz.

- Those dedicated to space research, Category B missions, specified in recommendation 401(2.4.17B) B-1. They are applicable to frequency bands 2290-2300 MHz and 8400-8450 MHz.

- Those dedicated to Earth exploration satellite missions, specified in recommendation 401(2.4.18) B-1. They are applicable to the frequency band 8025-8400 MHz.

- Those dedicated to space research, Category B missions, specified in recommendation 401(2.4.20B) B-1. They are applicable to the frequency band 31800-32300 MHz.

It should be noted that, stricto sensu, the above recommendations are applicable only to the mentioned frequency bands. However, the user should take note that extension to other SRS and/or EESS frequency bands could be envisaged in the future.

In no event will CCSDS or its members be liable for any incidental, consequential, or indirect damages, including any lost profits, lost savings, or loss of data, or for any claim by another party related to errors or omissions in this report.

1.3 REFERENCES

The following documents are referenced in this Report. At the time of publication, the editions indicated were valid. All documents are subject to revision, and users of this Report are encouraged to investigate the possibility of applying the most recent editions of the documents indicated below. The CCSDS Secretariat maintains a register of currently valid CCSDS documents.

[1] *Proceedings of the CCSDS RF and Modulation Subpanel 1E on Bandwidth-Efficient Modulations*. CCSDS B20.0-Y-2. Yellow Book. Issue 2. Washington, D.C.: CCSDS, June 2001.

[2] *Radio Frequency and Modulation Systems—Part 1: Earth Stations and Spacecraft*. Recommendation for Space Data System Standards, CCSDS 401.0-B-20. Blue Book. Issue 20. Washington, D.C.: CCSDS, April 2009.

[3] *Procedures Manual for the Consultative Committee for Space Data Systems*. CCSDS A00.0-Y-9. Yellow Book. Issue 9. Washington, D.C.: CCSDS, November 2003.

[4]   K. Murota and K. Hirade. "GMSK Modulation for Digital Mobile Radio Telephony."
      IEEE Transactions on Communications 29, no. 7 (July 1981): 1044-1050.

[5]   "NASA GSFC Efficient Spectrum Utilization Analysis." In *Proceedings of the CCSDS
      RF and Modulation Subpanel 1E on Bandwidth-Efficient Modulations*. CCSDS B20.0-
      Y-2. Yellow Book. Issue 2, 1-257–1-399. Washington, D.C.: CCSDS, June 2001.

[6]   J. Proakis and D. Manolakis. *Introduction to Digital Signal Processing*. New York:
      MacMillan, 1988.

[7]   G. Ungerboeck. "Channel Coding with Multilevel/Phase Signals." *IEEE Transactions
      on Information Theory* 28, no. 1 (January 1982): 55-67.

[8]   S.S. Pietrobon, et al. "Trellis-Coded Multidimensional Phase Modulation." *IEEE
      Transactions on Information Theory* 36, no. 1 (January 1990): 63-89.

[9]   M. Austin and M. Chang. "Quadrature Overlapped Raised-Cosine Modulation." *IEEE
      Transactions on Communications* 29, no. 3 (March 1981): 237-249.

[10] S. S. Shah, S. Yaqub, and F. Suleman. "Self-Correcting Codes Conquer Noise, Part
      One: Viterbi Codecs." *EDN* (February 15, 2001): 131-140.

[11] W. Martin, et al. 'CCSDS-SFCG Efficient Modulation Methods Study at NASA/JPL,
      Phase 4: Inteference Susceptibility'. In *Proceedings of the CCSDS RF and Modulation
      Subpanel 1E on Bandwidth-Efficient Modulations*. CCSDS B20.0-Y-2. Yellow Book.
      Issue 2, 1-171–1-212. Washington, D.C.: CCSDS, June 2001.

[12] G. Povero, E. Vassallo, and M. Visintin. 'Interference Susceptibility of Selected
      Bandwidth-Efficient Modulation Schemes'. In *Proceedings of the CCSDS RF and
      Modulation Subpanel 1E on Bandwidth-Efficient Modulations*. CCSDS B20.0-Y-2.
      Yellow Book. Issue 2, 1-473–1-492. Washington, D.C.: CCSDS, June 2001.

2   SCOPE OF BANDWIDTH-EFFICIENT MODULATIONS

2.1   LIMITED SPECTRAL RESOURCES FOR SPACE TELEMETRY

The Category A SRS frequency band 2200-2290 MHz is currently heavily used by space research and space operations missions for their telemetry transmissions, and the density of users of the band keeps increasing over the years. In addition, while until recently all these users were rather modest in telemetry symbol rate transmission, more and more new missions are appearing with telemetry symbol rates well above 1 Ms/s. In order to avoid a rapid saturation of the band with unsolvable interference conflicts, the CCSDS has issued a recommendation 401(2.4.17A) for a limited set of common bandwidth-efficient modulation schemes to be used for high symbol rate transmissions, thus ensuring not only an optimum use of the band but also inter-agency cross-support capability. The recommendation is also applicable to the 8450-8500 MHz band for which a number of missions with high rate telemetry have already been earmarked.

Likewise, recommendation 401(2.4.17B) B-1 addresses the Category B SRS bands 2290-2300 MHz and 8400-8450 MHz, while recommendation 401(2.4.20B) B-1 addresses the 31.8-32.3 GHz Category B SRS band. These recommended modulations have been selected for their low loss and their bandwidth compactness.

Recommendation 401(2.4.18) B-1 addresses the EESS payload telemetry bands 8025-8400 MHz and 25.5-27 GHz. The band available at 8 GHz is only 375 MHz while some EESS missions are under preparation plan to transmit hundreds of Megabits per second of payload data leading to channel symbol rates possibly up to 1 Gs/s. The problem is two-fold: the physical limitation of the band in terms of transmission rate capacity and the increased risk of interference. CCSDS policy as expressed in recommendation 401(2.4.18) is to promote the use of a very compact modulation scheme for use in the 8 GHz band and to encourage the very high rate users to migrate to the 26 GHz band.

2.2   REGULATIONS: THE SFCG SPECTRAL MASK

The SFCG was established to provide a less formal and more flexible environment, compared to the official organs of the ITU, for the solution of frequency management problems encountered by member space agencies. Recognizing that the SRS and EESS frequency bands were increasingly congested and concerned with the effective use of those bands, the SFCG approved Recommendation 17-2R1 in 1999 which established spectral emission limits for space-to-Earth links in the space science services. Separate spectral emissions masks were established for missions with telemetry data rates less than 2 Ms/s and for those with data rates greater than 2 Ms/s.

In September of 2003, the 17-2R1 mask was modified and renumbered 21-2R2 for Category A bands 2200-2290 MHz, 8025-8400 MHz, and 8450-8500 MHz. SFCG Recommendation 23-1 was also approved in September of 2003, providing guidance on the maximum allowable bandwidth as a function of data rates for space-to-Earth links in the Category B

bands 2290-2300 MHz and 8400-8450 MHz. The SFCG Recommendations currently in-force can be found at the SFCG website http://www.sfcgonline.org/.

2.3   A SELECTION OF BANDWIDTH-EFFICIENT MODULATION METHODS

The selection of modulations schemes is the result of compromises on a number of criteria:

– bandwidth efficiency;

– link performances (in terms of BER);

– implementation complexity and cost: onboard transmitter, ground receiver;

– robustness: susceptibility to interferers;

– programmatic aspects: cross-compatibility.

2.3.1   MODULATION METHODS FOR SRS, CATEGORY A

Because of the wide range of applications, ranging from the low-Earth orbiters to the science spacecraft at the edge of the Category A region (2×10^6 km), a number of different modulation schemes were retained in recommendation 401(2.4.17A) B-1:

– GMSK[2] (BT_s=0.25) with precoding;

– Filtered OQPSK[2] with various options:

  • Baseband SRRC[2], α=0.5;

  • Baseband Butterworth 6 poles, BT_s=0.5;

  • Other types of bandpass filters provided that the equivalent baseband BT_s is not greater than 0.5 and they ensure compliance with SFCG Recommendation 21-2R2 (or latest version) and interoperability with cross-supporting networks.

2.3.2   MODULATION METHODS FOR SRS, CATEGORY B

For SRS Category B missions, only one modulation was retained in recommendation 401(2.4.17B) B-1 and recommendation 401(2.4.20B) B-1:

– GMSK[2] (BT_s=0.5) with precoding.

---

[2]These terms are defined in sections 3 and 4.

2.3.3   MODULATION METHODS FOR EESS AT 8 GHZ

Recommendation 401(2.4.18) B-1 contains three modulation options recommended for EESS missions:

– 4D 8PSK TCM;[2]

– GMSK[2] (BT_s=0.25) with precoding;

– Filtered OQPSK[2] with various options:

  • Baseband SRRC[2], α=0.5;

  • Baseband Butterworth 6 poles, BT_s=0.5;

  • Other types of bandpass filters provided that the equivalent baseband BT_s is not greater than 0.5 and they ensure compliance with SFCG Recommendation 21-2R2 (or latest version) and interoperability with cross-supporting networks.

2.4   BIT AND SYMBOL RATE TERMINOLOGY

In the literature, the notations used for bit rate and symbol rate sometimes have different meanings. For this Green Book, R_b refers to the information bit rate and R_{ChS} refers to the channel symbol rate after the modulator. R_s is used to denote the coded symbol rate measured at the input of the modulator. If no error correcting coding nor Bi-ϕ formatting is used, then R_s is equal to the information bit rate R_b. Likewise, T_b is the bit period, T_s is the coded symbol period, and T_{ChS} is the channel symbol period. If there is no error correcting coding nor Bi-ϕ formatting, $T_s = T_b$.

Figure 2-1 shows the relationship between the different terms.
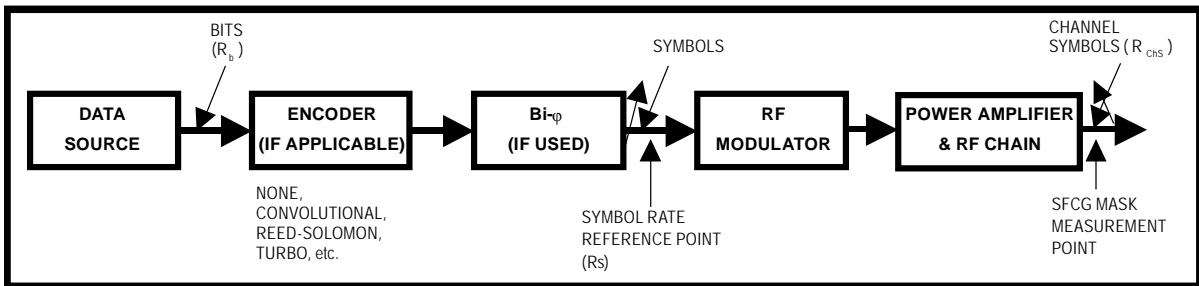
Figure 2-1: Bit and Symbol Rate Terminology

3   TECHNICAL DEFINITIONS

3.1   PRECODED GMSK

3.1.1   INTRODUCTION

Gaussian Minimum Shift Keying (GMSK) is a constant envelope, continuous phase modulation first introduced in 1981 by Murota and Hirade (reference [4]). It is derived from Minimum Shift Keying (MSK) with the addition of a baseband Gaussian filter that further reduces sidelobe levels and spectral bandwidth.   The product of the Gaussian filter bandwidth and the coded symbol period at the input to the modulator, referred to as the BT_s factor, is used to differentiate between GMSK modulations of varying bandwidth efficiencies. If there is no coding, BT_s refers to the filter bandwidth times the bit period.[3] In general, a smaller BT_s factor results in less spectral bandwidth occupancy but greater intersymbol interference which can be compensated for using equalization or trellis demodulation. GMSK has a constant envelope which reduces spectral regrowth and signal distortion due to amplifier nonlinearity.

Like MSK, GMSK is inherently a differential Continuous Phase Modulation (CPM) (i.e., the information is carried in the change of the phase rather than the phase itself). For a coherent in-phase/quatrature (I/Q) demodulator, at the receiver is needed a differential decoder which increases the BER by approximately a factor of two. By precoding the GMSK signal at the transmitter to remove the inherent differential encoding, the BER can be halved. Figure 3-1 shows a block diagram of the precoder were $d_k \in \{\pm 1\}$.
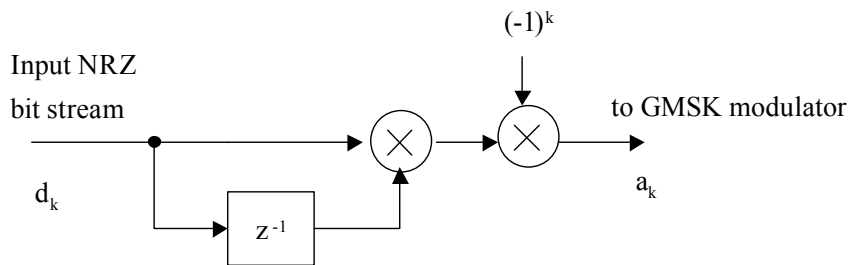
Figure 3-1: GMSK Precoder

3.1.2   SIGNAL MODEL

Mathematically, the precoded GMSK modulated RF carrier is expressed as:

$$x(\tau) = \sqrt{2P} \cos\left(2\pi f_c \tau + \varphi(\tau) + \varphi_0\right)$$

where:
   P is the power of the carrier;
   f_c is the center frequency;

---

[3] See 2.4 for bit/symbol terminology definitions used in this Green Book.

$\varphi(\tau)$ is the phase of the modulated carrier;

φ_0 is a constant phase offset;

and

$$\varphi(t) = \sum_k (a_k \frac{\pi}{2} \int_{-\infty}^{t-kT_s} g(\tau) d\tau)$$

where $a_k = (-1)^k d_k d_{k-1}$ are the pre-coder output symbols and $d_k \in \{\pm 1\}$ is the k-th coded symbol to be transmitted.

The instantaneous frequency pulse $g(\tau)$ can be obtained through a linear filter with impulse response defined by:

$$g(\tau) = h(\tau) * rect(\tau/T_s)$$

where * denotes convolution and *rect(x)* is the function:

$$rect(\tau/T_s) = 1/T_s \text{ for } |\tau| < T_s/2$$
$$rect(\tau/T_s) = 0 \quad \text{otherwise}$$

and *h(t)* is the Gaussian filter impulse response:

$$h(t) = \frac{1}{\sigma T_s \sqrt{2\pi}} e^{-\frac{t^2}{2\sigma^2 T_s^2}}$$

where

$$\sigma = \frac{\sqrt{\ln(2)}}{2\pi B T_s}$$

and

$\ln(\bullet)$ is the natural logarithm (base $= e$)

B = one-sided 3-dB bandwidth of the filter with impulse response $h(t)$

T_s = the duration of a coded symbol at the input to the modulator

3.1.3 GMSK MODULATOR

3.1.3.1 General

There are two common methods of generating GMSK, one as a Frequency Shift Keyed (FSK) modulation and the other as an offset quadrature phase shift keyed modulation. Figure 3-2 shows GMSK generated as an FSK modulation using a Voltage Controlled Oscillator (VCO) as first described in reference [4]. Figure 3-3 shows GMSK generated using a quadrature baseband method.

Figure 3-2 shows the simulated spectrum of GMSK BT_s=0.25 and BT_s=0.5 at the output of the saturated SSPA referenced in annex B. The SFCG Recommendation 21-2 spectral high data rate mask is also plotted, and it can be clearly seen that GMSK with either BT_s factor meets the requirements of the mask.

NRZ
precoded
bit stream ⟶ Gaussian LPF ⟶ VCO ⟶ to RF amplifier

a_k
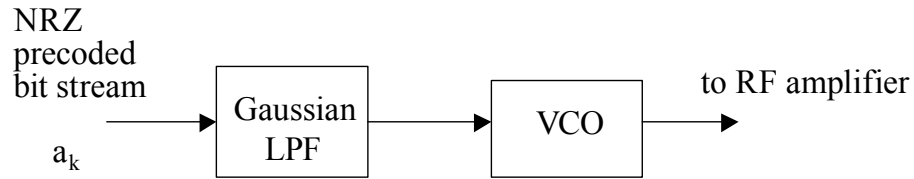
Figure 3-2: GMSK: Generated Using VCO

NRZ
precoded
bit stream ⟶ Gaussian LPF ⟶ ∫ dt ⟶ sin (•) ⟶ ⊗   cos(•) ⟶ ⊗   OSC   90°   ⊕ ⟶ to RF amplifier
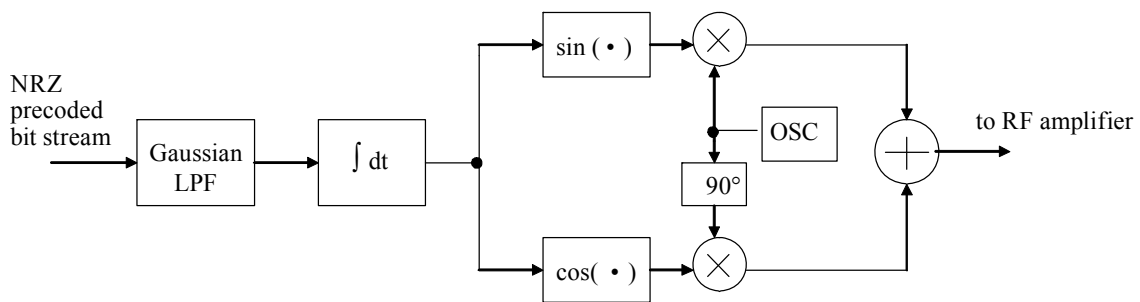
Figure 3-3: GMSK Using a Quadrature Modulator
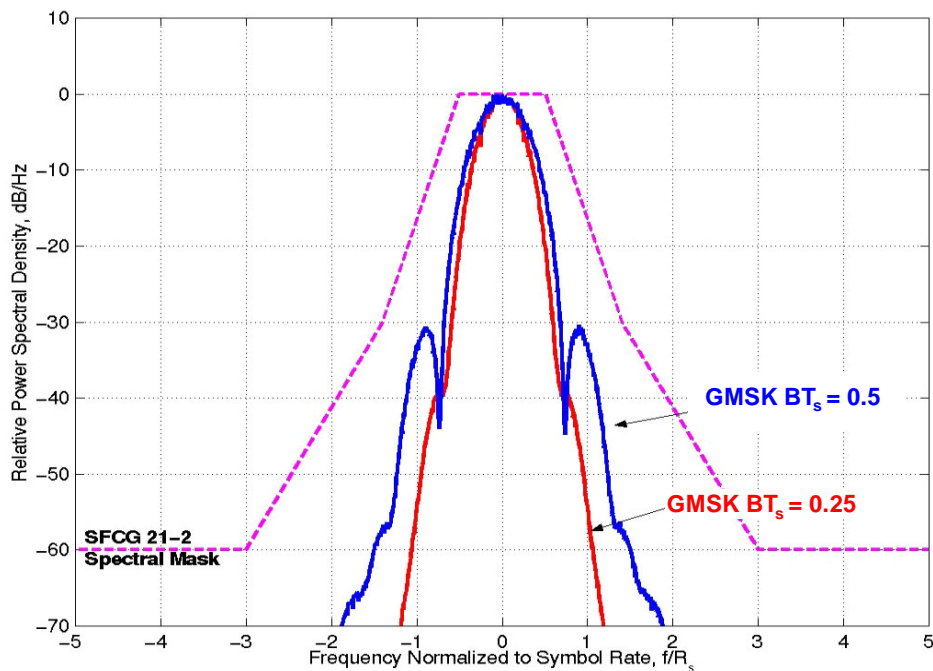
Figure 3-4: Simulated GMSK Spectrum at Output of Saturated SSPA

3.1.3.2 Symbol Asymmetry in Analog GMSK Transmitters

The analog transmitter implementations shown in figures 3-2 and 3-3 may suffer from the impairment known as data asymmetry, i.e., unequal rise and fall times of the logic gating circuits which generate the input NRZ signal (see figure 3-5). With symbol asymmetry, the positive-to-negative transitions occur at time instants $kT_s \pm \eta T_s$ instead of kT_s. The discussions below assume the case of $kT_s + \eta T_s$.
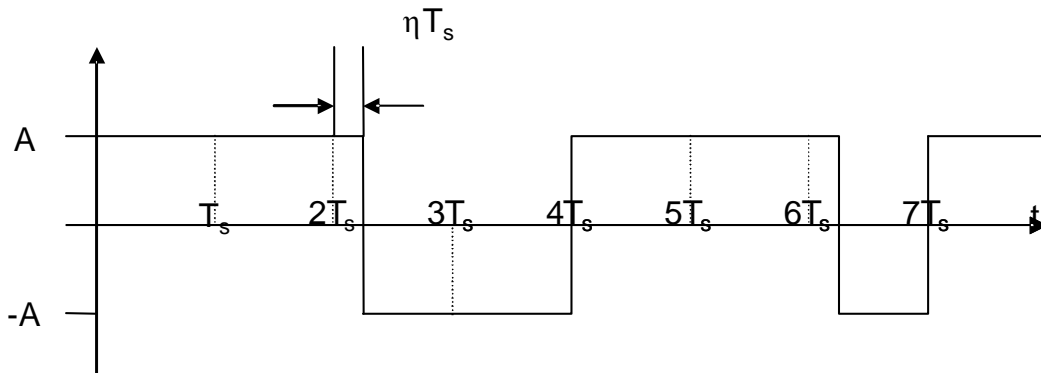
Figure 3-5: NRZ Signal Affected by Symbol Asymmetry (η=0.25)

In the presence of symbol asymmetry, the mean value of the NRZ signal is equal to $2\eta Ap$, where p is the probability that a negative-going transition occurs. If the positive and negative levels are equally likely (i.e., no data imbalance) and $p=1/4$, the NRZ signal mean value is $\eta A/2$. The signal at the output of the modulator has an instantaneous frequency deviation $f(t)=d\varphi(t)/dt$ with an average value $\mu_f=\eta/8T_s$, so its true center frequency is $f_c+\mu_f$ instead of f_c. The receiver carrier phase synchronizer is able to compensate for the frequency offset as long as its loop bandwidth B_L is larger than μ_f. However, intersymbol interference due to symbol asymmetry cannot be eliminated, and the resulting loss can be measured in terms of signal-to-noise ratio necessary for given BER. For $\eta \leq 0.002$, the E_s/N_o degradation at the output of the GMSK receiver is lower than 0.1 dB.
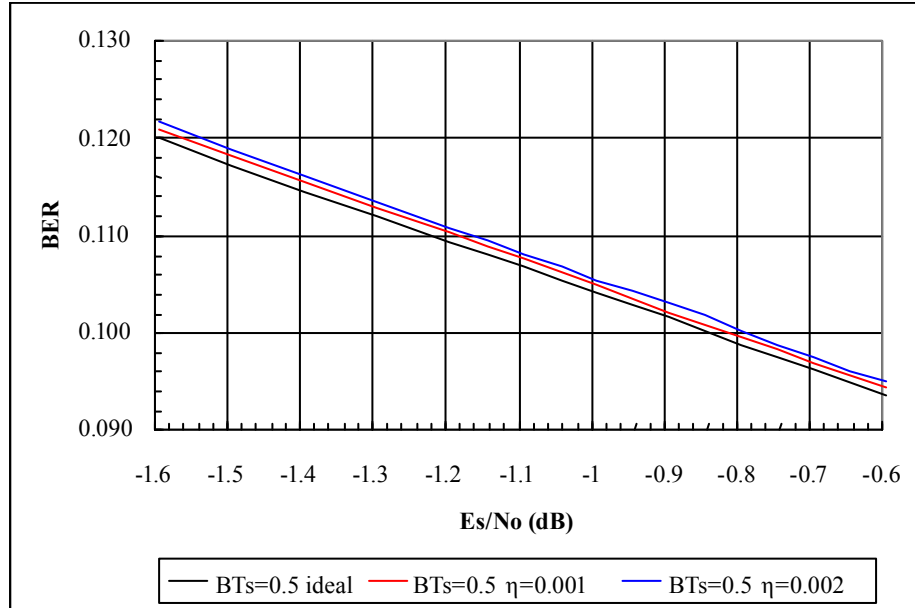
Figure 3-6: Bit Error Rate (BER) at the Output of the GMSK Receiver in the Presence of Data Asymmetry; Case of BT_s=0.5
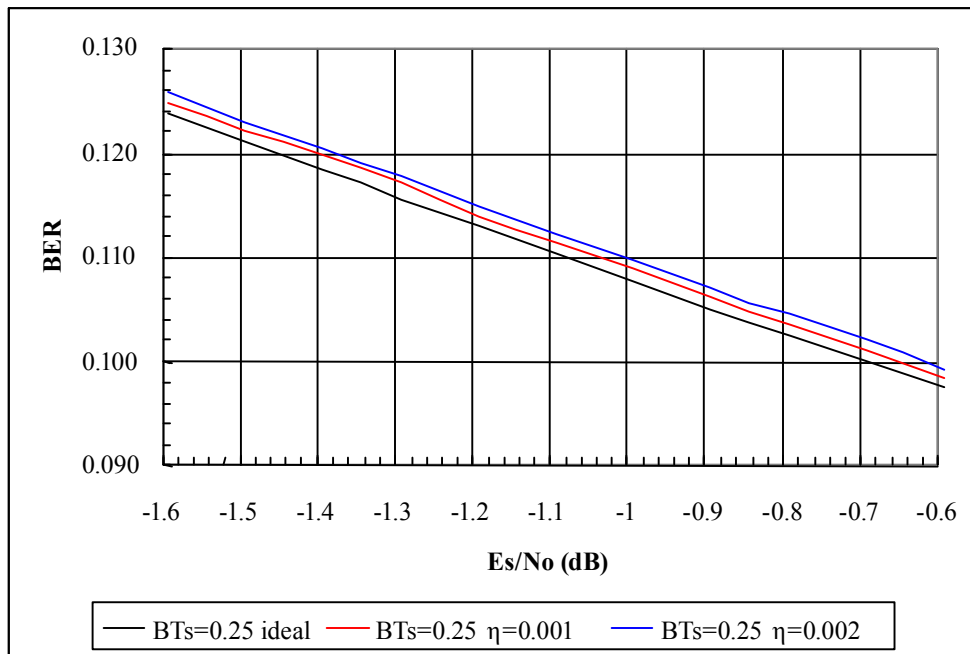
Figure 3-7: Bit Error Rate (BER) at the Output of the GMSK Receiver in the Presence of Data Asymmetry; Case of BT_s=0.25

3.1.3.3 Carrier Phase/Amplitude Imbalance in Quadrature GMSK Transmitters

In the quadrature GMSK modulator, two orthogonal sinusoidal signals are generated from one oscillator, using a $\pi/2$ phase shifter. The presence of carrier phase/amplitude imbalance due to implementation gives rise to spectral lines in the power spectrum of the transmitted signal and BER degradation at the receiver output. Simulations showed that the coherent receiver finds its stable phase reference at $\theta/2$ and that the loss due to increased intersymbol interference is negligible as long as θ is less than 5° and the amplitude imbalance is lower than 0.5 dB (see figure 3-8).
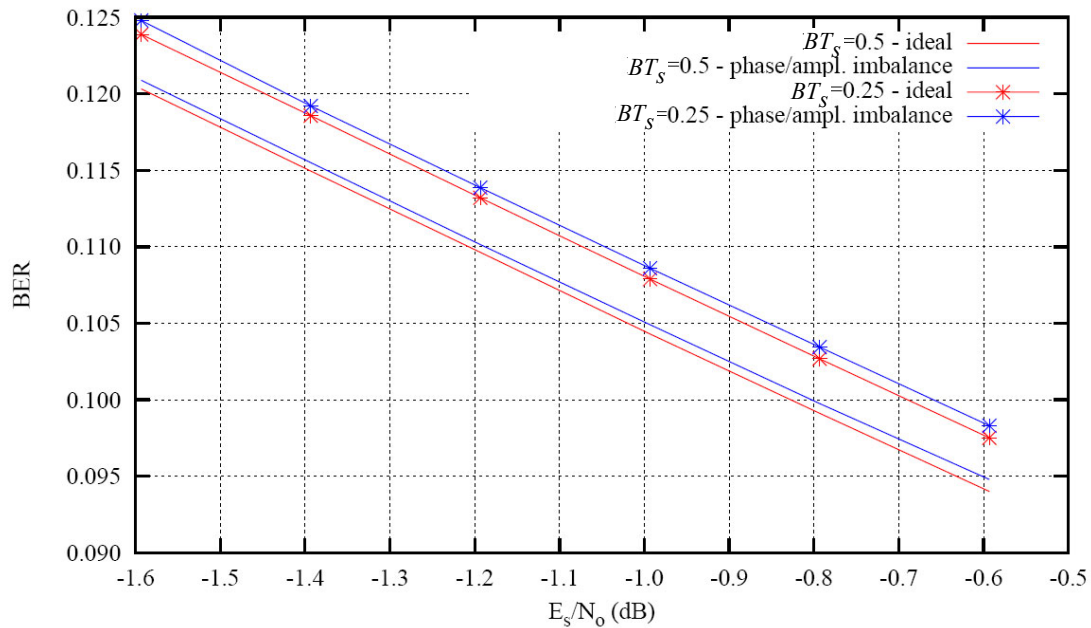
Figure 3-8: Bit Error Rate (BER) at the Output of the GMSK Receiver in the Presence of Carrier Phase/Amplitude Imbalance

3.1.3.4 Parameters to be Used in Digital GMSK Transmitters

Full digital transmitters may be developed, based on the schemes of figures 3-2 and 3-3. The NRZ signal is sampled using N_b samples per coded symbol at the input to the modulator, and an FIR filter with impulse response $h[n]$ is used instead of the analog Gaussian filter. This type of transmitter is denoted here as FM-2 if the VCO is present (figure 3-2) and IQ-2 if the IQ transmitter is present (figure 3-3). The value of N_b, the number of taps N_T of the FIR filter, and the number of quantization bits N_q to be used in the FIR filter must be found so that the introduced approximations in the transmitted signal are negligible. Another possibility, which shall be called FM-1, is shown in figure 3-9. In this case, the NRZ input signal is sampled using one sample per bit. An oversampler introduces N_b-1 zeros between the two input samples and generates a train of discrete deltas which feed an FIR filter with impulse response $g[n]$. In figure 3-9 the digital-to-analog conversion is placed right after the

FIR filter because an analog VCO is used, but a numerically controlled oscillator can be used instead. Moreover, a quadrature modulator may be used instead of the VCO, as in figure 3-3.
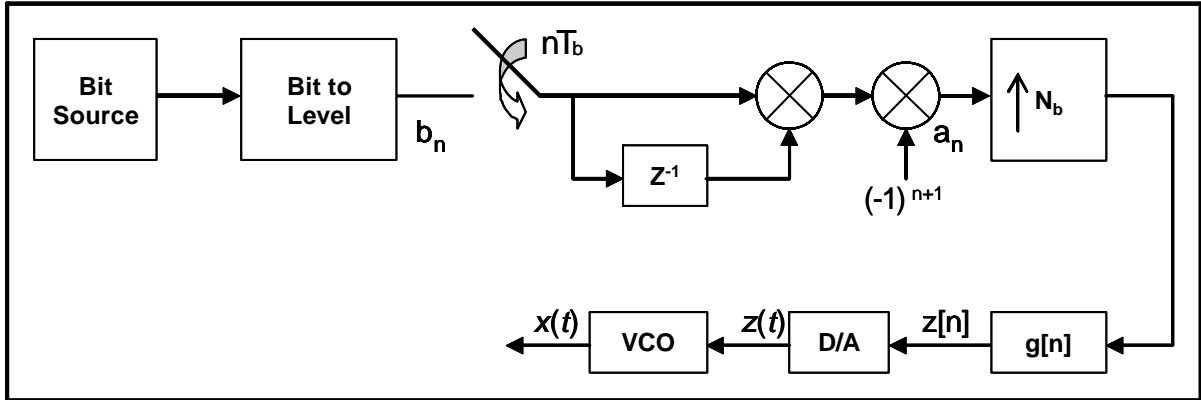
Figure 3-9: The FM-1 Implementation of the Precoded GMSK Transmitter

Another quadrature modulator (IQ-L1) can be designed, based on the Laurent decomposition of the GMSK signal complex envelope (see figure 3-11):

$$\tilde{x}(t) \approx A_c \sum_{n=-\infty}^{\infty} [b_{2n} C_0 (t - 2nT_s) - b_{2n+1} b_{2n} b_{2n-1} C_1 (t - 2nT_s - T_s)]$$

$$+ jA_c \sum_{n=-\infty}^{\infty} [b_{2n+1} C_0 (t - 2nT_s - T_s) - b_{2n} b_{2n-1} b_{2n-2} C_1 (t - 2nT_s)]$$

where $C_0(t)$ and $C_1(t)$ are shown in figure 3-10 for $BT_s = 0.5$ and $BT_s = 0.25$.
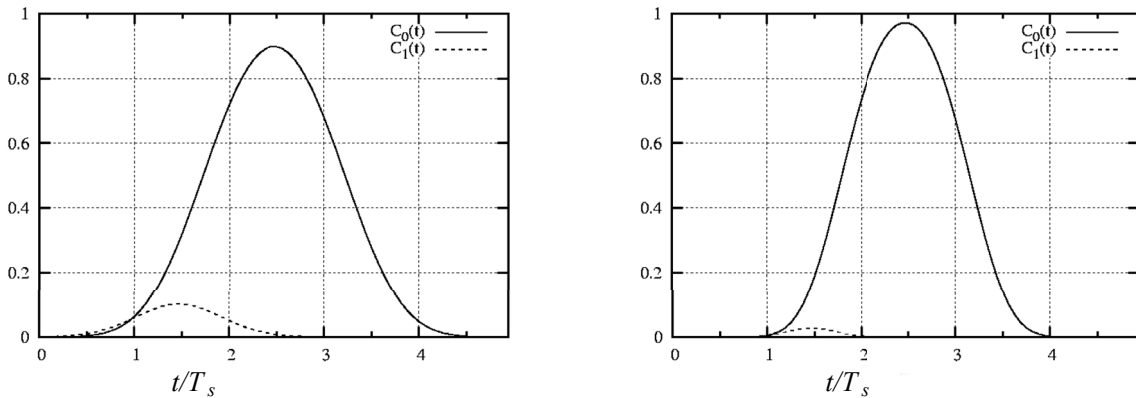
Figure 3-10: Pulses C0(t) and C1(t) with $BT_s = 0.25$ (left) and $BT_s = 0.5$ (right)
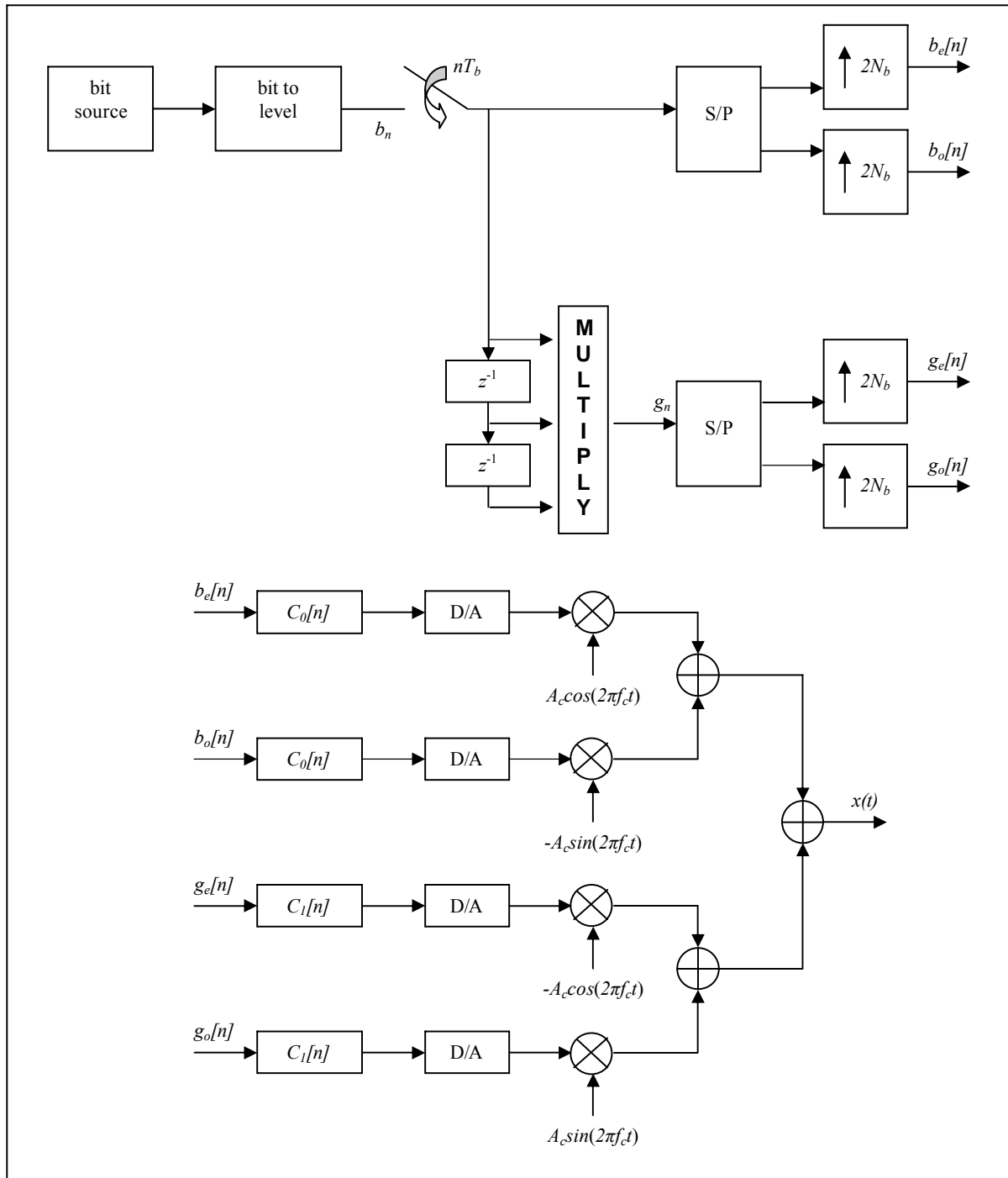
Figure 3-11: IQ-L1 Implementation of the Transmitter

The complex envelopes of the signals generated with transmitter of figure 3-11 using only one amplitude (AMP) component (only $C_0(t)$) or both components are shown in figures 3-12 and 3-13 for $BT_s=0.5$ and $BT_s=0.25$, respectively. The use of both components is needed for GMSK with $BT_s=0.25$, while one component is sufficient for the generation of the GMSK signal with $BT_s=0.5$.
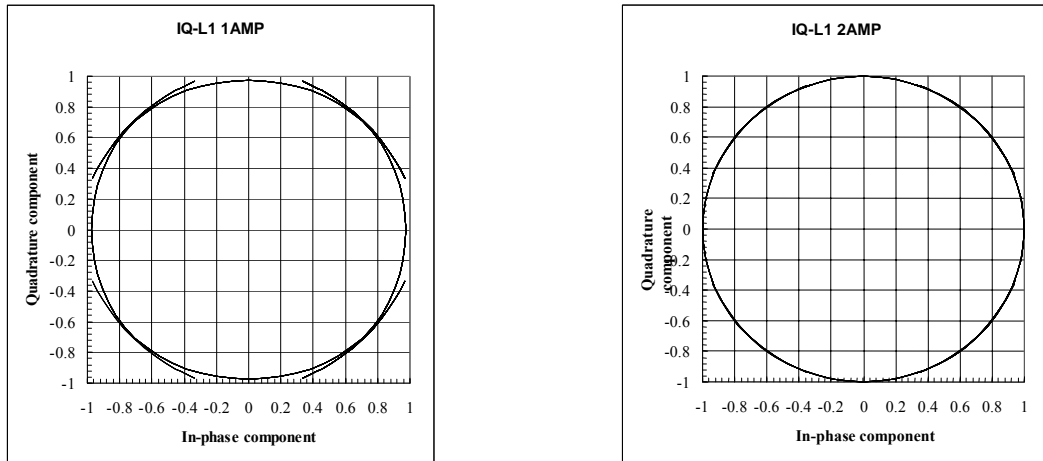
Figure 3-12: Scattering Diagram for the IQ-L1 Implementation with 1 and 2 Amplitude Components; GMSK with BT_s=0.5
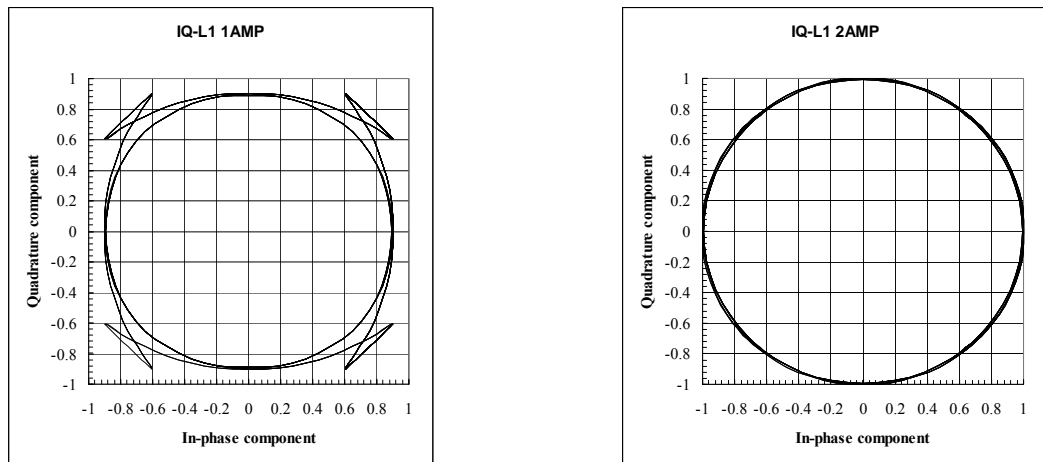
Figure 3-13: Scattering Diagram for the IQ-L1 Implementation with 1 and 2 Amplitude Components; GMSK with BT_s=0.25

The parameters that give negligible distortions in the transmitted signal are presented here. For BT_s=0.25, $N_b \geq 4$ and $N_q \geq 12$ are needed for all the implementations. For BT_s=0.5, $N_b \geq 4$ and $N_q \geq 12$ are needed for the IQ-L1 transmitter, while $N_b \geq 4$ and $N_q \geq 16$ are needed for the other implementations. In order to correctly implement the Gaussian filter, the number of taps N_T must be at least $5N_b$ for GMSK with BT_s=0.25, and at least $4N_b$ for GMSK with BT_s=0.5. For the filter with impulse response $g[n]$, the number of taps N_T must be at least $6N_b$ for GMSK with BT_s=0.25, and at least $5N_b$ for GMSK with BT_s=0.5. For the filter with impulse response $C_0[n]$, the number of taps N_T must be at least $4N_b$ for GMSK with BT_s=0.25 and 0.5, while $C_1[n]$ requires $2N_b$ taps. Figures 3-14 and 3-15 show the eye patterns of the signals at the output of the receiver filter (in-phase component) for pre-coded GMSK with

BT_s=0.5 and BT_s=0.25. The intersymbol interference present in the case BT_s=0.25 may be reduced by including a 3-tap equalizer (Wiener filter) with weights $w_0 = w_2 = -0.0859984, w_1 = 1.0116342$ and delay equal to $2T_s$ between taps. The eye pattern at the output of the equalizer is shown in figure 3-16. The simulated power spectra obtained with an FM-2 implementation and with an IQ-L1 implementation with the above parameters are shown in figures 3-17 and 3-18.
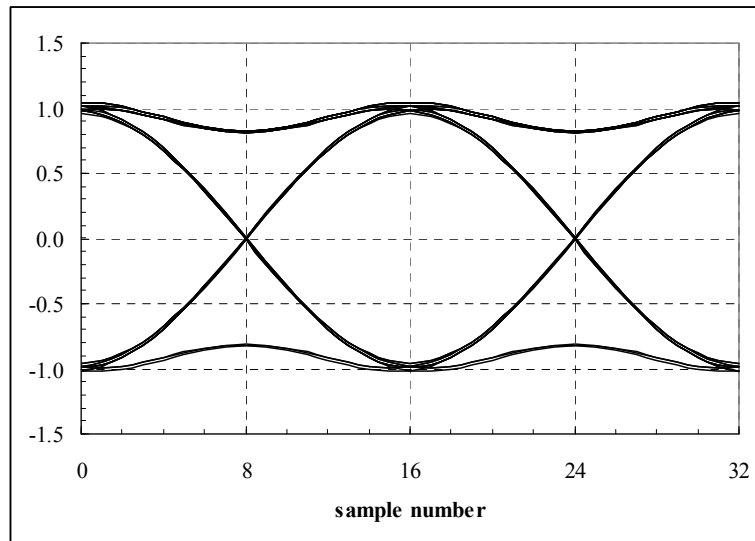
Figure 3-14: Eye Pattern at the Output of the Receiver Filter for GMSK with BT_s=0.5
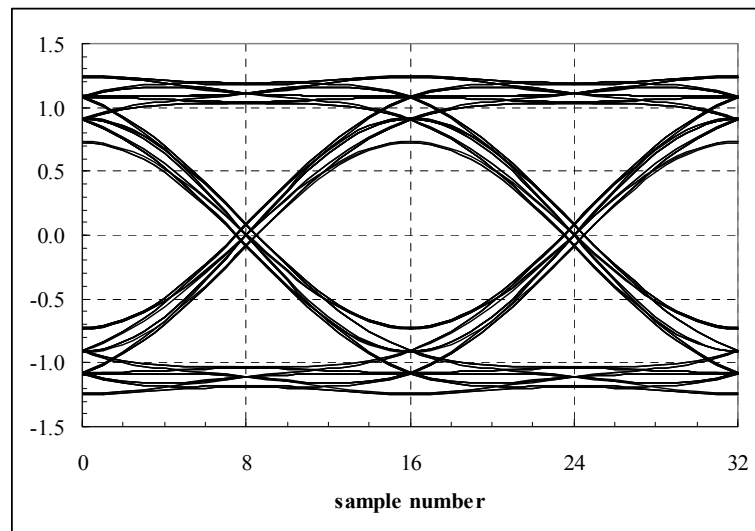
Figure 3-15: Eye Pattern at the Output of the Receiver Filter for GMSK with BT_s=0.25
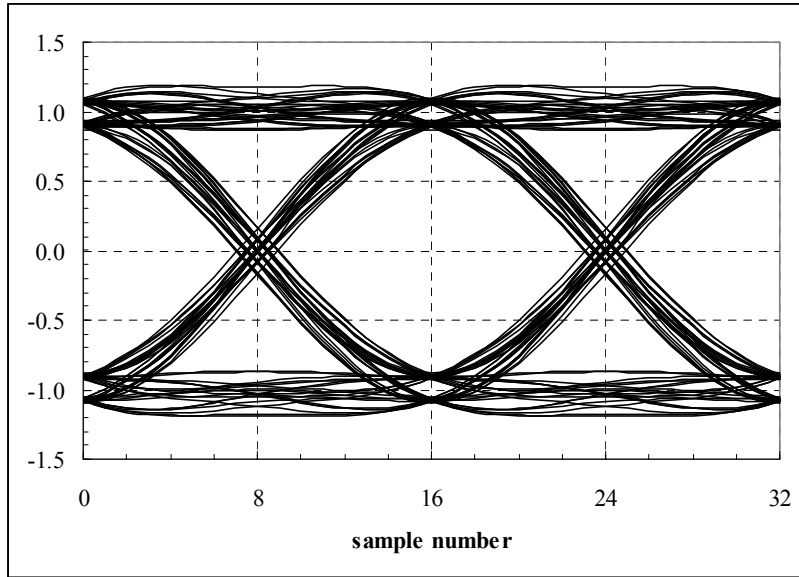
Figure 3-16: Eye Pattern at the Output of the Wiener Equalizer for GSMK with BT_s=0.25
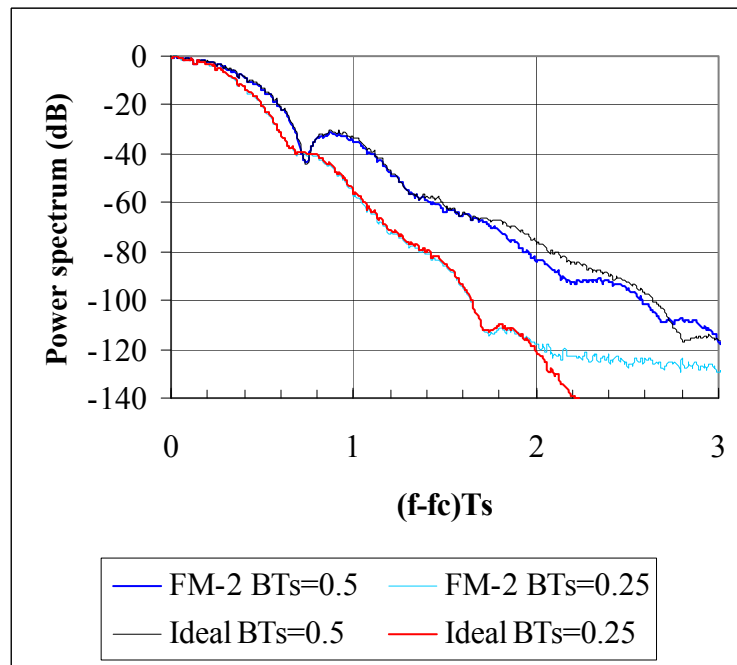
Figure 3-17: Comparison of the GMSK BT_s=0.5 Power Spectra Obtained with an Ideal Transmitter and an FM-2 Transmitter
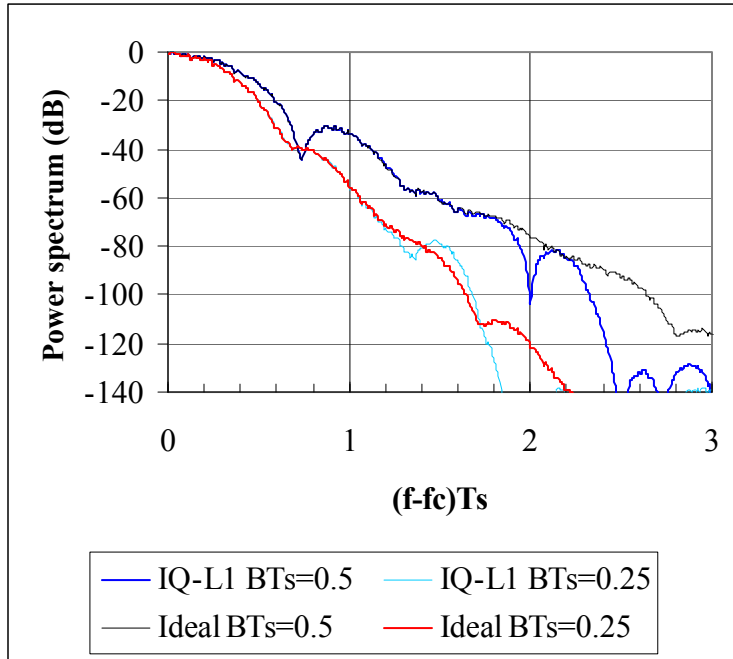
Figure 3-18: Comparison of the GMSK BT_s=0.5 Power Spectra Obtained with an Ideal Transmitter and an IQ-L1 Transmitter

3.2 FILTERED OFFSET-QPSK

3.2.1 INTRODUCTION

Offset-QPSK (OQPSK) is a proven modulation technique which is robust and easily implemented. OQPSK receivers, typically employing integrate-and-dump type demodulators, are widely deployed by several international space agencies at ground stations operating downlinks in the S-band and X-band frequencies. With the use of proper filtering techniques, OQPSK modulation can meet the out-of-band emissions requirements of SFCG Recommendation 21-2R2 while still providing good BER performance with existing OQPSK receivers.

The majority of CCSDS studies performed on filtered OQPSK have examined baseband filtered implementations using Butterworth and Square Root Raised Cosine (SRRC) filters. These implementations avoid the additional cost, weight, and power loss (insertion loss plus filtering loss) associated with the use of RF filters, and have been shown to have good performance. However, filtered OQPSK with other filter types (including post-modulation filters) can also meet the high rate SFCG spectral mask requirements. This subsection details baseband filtered OQPSK implementations.

Two implementations of baseband filtered OQPSK modulation are described below: OQPSK with an I/Q modulator and OQPSK with a linear phase modulator, referred to as OQPSK/PM. Baseband filtered OQPSK with an I/Q modulator, filters the I and Q channel NRZ data signals and multiplies the filtered signals with in-phase and quadrature carrier

signals. The baseband filtered OQPSK/PM signal is formed by mapping the I and Q NRZ data to a four-state phase signal, filtering the phase signal and then phase modulating a carrier with the filtered phase signal.

As with all modulations, the actual BER performance of filtered OQPSK is dependent on the receiver detection method used. An integrate-and-dump receiver with symbol-by-symbol detection is mathematically optimal for unfiltered OQPSK waveforms only. For filtered OQPSK, without the use of a complex maximum-likelihood receiver, the optimal receiver design would employ a receive filter precisely matched to the transmitter filter and an equalizer to remove intersymbol interference. For a modulation technique in which multiple alternative filter types have been recommended, this may seem to be a problem. Fortunately, in practice an integrate-and-dump filter receiver will provide good performance for most types of filtered OQPSK including those recommended.

Subsection 3.2.2 describes in detail the I/Q and linear phase modulator implementations of baseband filtered OQPSK. Subsection 3.3.3 presents various filtering options, including simulated power spectral density plots for three filter types.

3.2.2   MATHEMATICAL DEFINITION AND IMPLEMENTATION

Two modulator forms are commonly used for implementation of baseband filtered OQPSK (reference [5]). The linear phase modulator implementation is described in 3.2.2.1 and the I/Q modulator implementation is described in 3.2.2.2.[4]

3.2.2.1   Baseband Filtered OQPSK Linear Phase Modulator

OQPSK/PM uses a linear phase modulator to map a filtered phase signal onto the carrier. This configuration is shown in figure 3-19.
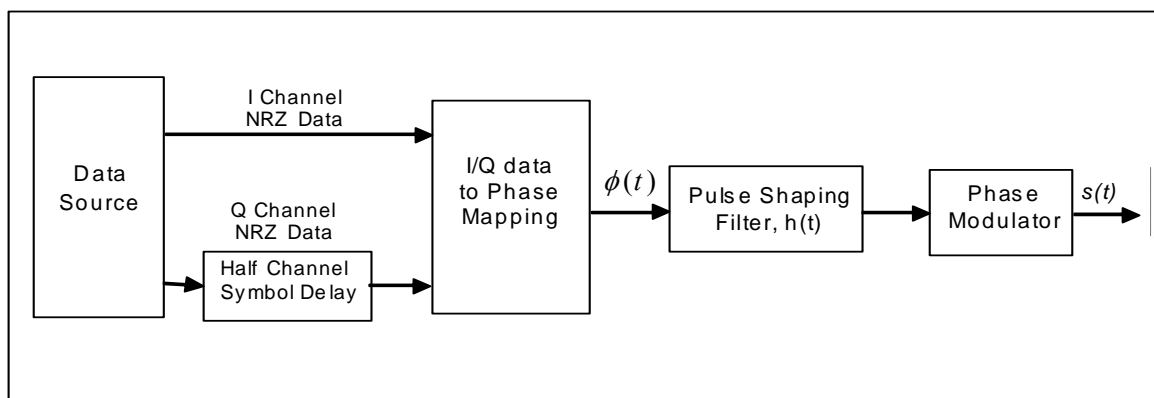
Figure 3-19: Filtered OQPSK with Linear Phase Modulator (OQPSK/PM)

---

[4] See 2.4 for bit/symbol terminology definitions used in this Green Book.

The input to the modulator is the in-phase (I) and Quadrature (Q) NRZ data streams. The Q-channel data stream is delayed by ½ symbol to create offset QPSK. The I and Q data is mapped to a phase signal which then goes through a pulse shaping filter.[5] This is then used as an input to a linear phase modulator to produce the modulated output signal. The output of the modulator can be expressed as:

$$s(t) = \sqrt{2P} \cos(2\pi f_c t + \phi(t) * h(t))$$

where

P = carrier power

f_c = carrier frequency

$\phi(t)$ is the phase output from the I-Q to phase mapping

$h(t)$ is the impulse response of the pulse shaping filter

* denotes convolution

The phase modulator implementation of baseband filtered OQPSK produces a constant envelope signal, as can be seen in the phasor diagrams in figure 3-20. The constant envelope property of the signal is important because this will reduce the impact of the nonlinear AM/AM and AM/PM distortion of the saturated transmitter power amplifier.

Butterworth Filter, $BT_s = 0.5$ SRRC Filter, Alpha = 0.5
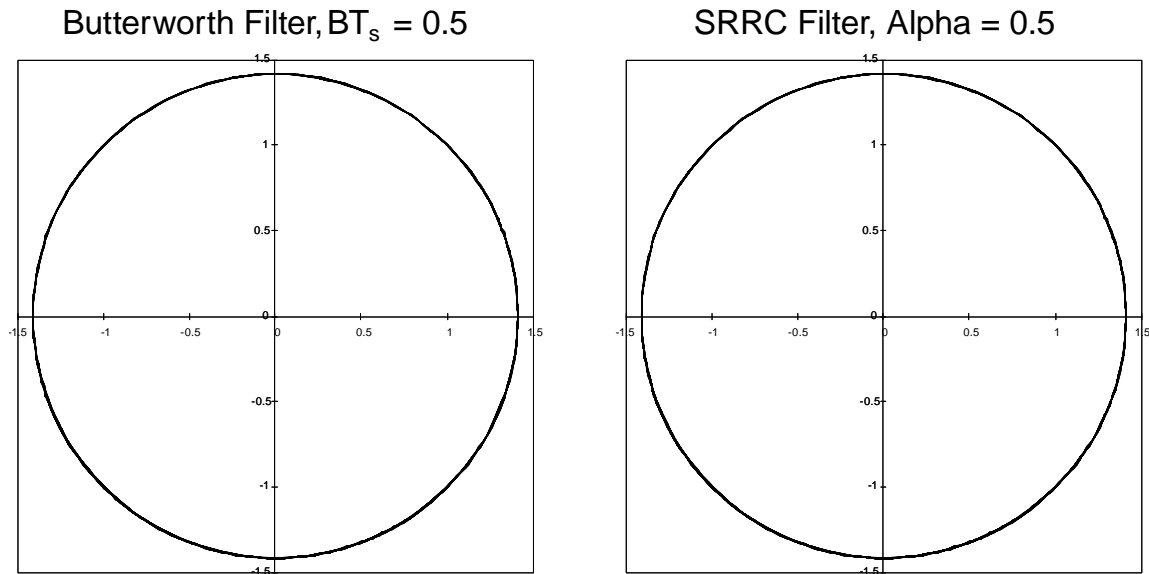
Figure 3-20: Baseband Filtered OQPSK/PM Implementation Phasor Diagrams

---

[5] Discrete spectral lines may be avoided if phase mapper uses the minimum phase rotation during transitions from one phase to another, e.g. +90° instead of -270°.

3.2.2.2 Baseband Filtered OQPSK I/Q Modulator

The second OQPSK implementation uses an I/Q modulator where the in-phase and quadrature carrier signals are amplitude modulated with a filtered NRZ data stream. This implementation is illustrated in figure 3-21.
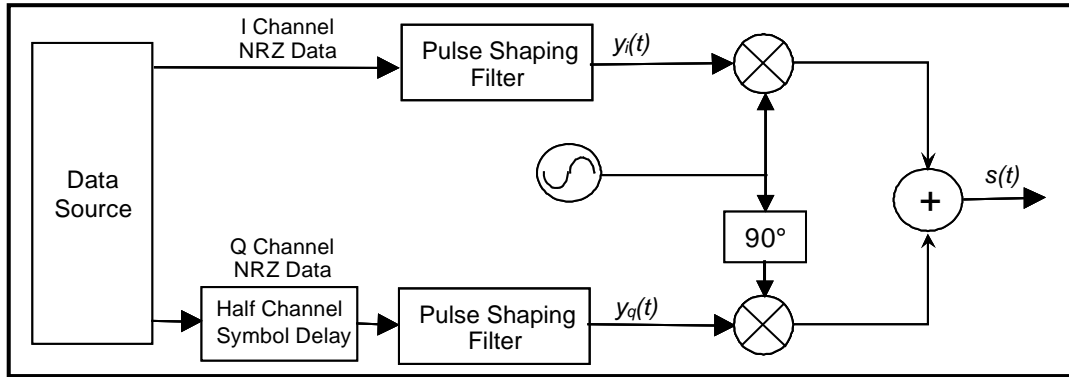
Figure 3-21: Baseband Filtered OQPSK with I/Q Modulator

The input to the modulator is the I and Q NRZ data streams. The Q-channel data stream is delayed by half a channel symbol to create Offset QPSK. The output of the modulator can be expressed as:

$$s(t) = y_i(t)\sin(2\pi f_c t + \varphi) + y_q(t)\cos(2\pi f_c t + \varphi)$$

where $y_i(t)$ and $y_q(t)$ are filtered NRZ data and φ is the initial oscillator phase.

In this implementation, the magnitude variations due to filtering are present in the output signal and thus the output signal does not have a constant envelope. This is evident in the phasor diagrams in figure 3-22. As a result, this implementation will cause spectral regrowth and Inter-Symbol Interference (ISI) when used with a non-linear power amplifier.

Butterworth Filter, $BT_s = 0.5$ SRRC Filter, $\alpha = 0.5$
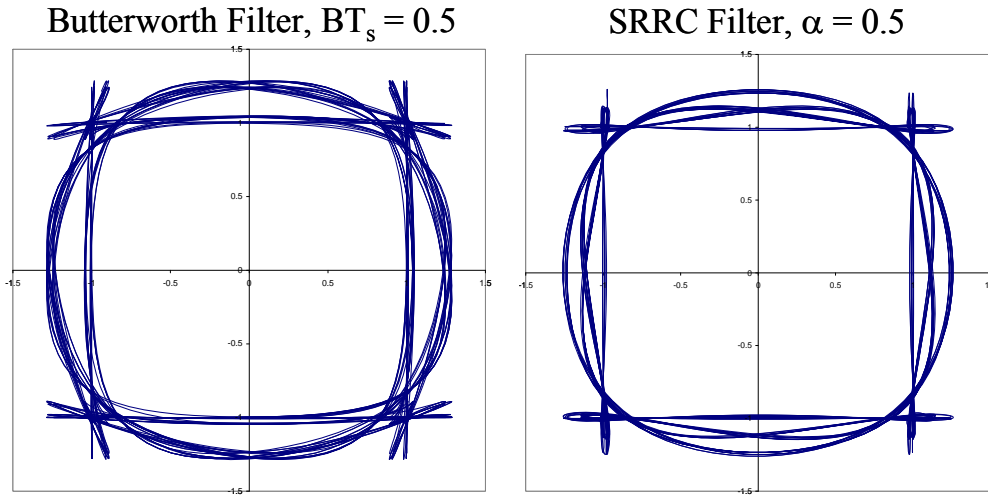
Figure 3-22: Baseband Filtered OQPSK I/Q Implementation Phasor Diagrams

In the absence of filtering, the implementations shown in figures 3-19 and 3-21 produce identical output signals.

3.2.2.3   Baseband Filtering Techniques

This subsection describes the characteristics of three example baseband filters that can be used with OQPSK modulation to meet the spectral containment requirements of the SFCG mask. The optimal filter type and parameters for any given system are a function of the receiver type and the particular distortion characteristics of that system. However, a number of defined filter types with standard parameters have been shown to provide generally good spectral containment and power efficiency performance and are thus specifically identified in the CCSDS recommendation.   The two filters specifically mentioned are a 6th order Butterworth filter ($BT_s = 0.5$) and a Square Root Raised Cosine filter ($\alpha = 0.5$). B is defined as the one-sided 3-dB filter bandwidth and T_s is the coded symbol period (or bit period if uncoded) at the input to the modulator.

Extensive simulation analyses have been performed on baseband filtered OQPSK using these two filter types. These analyses, which employed an integrate-and-dump type OQPSK demodulator and included the effects of hardware distortions typical of SRS missions, form the basis for the recommendation of this modulation technique. A limited number of additional analyses have also been performed using other filter types such as Bessel, Raised Cosine, and Chebyshev filters. These simulations have shown that good power and spectral containment performance can be realized with alternative filter types as well.

This subsection provides the characteristics of the filter types recommended for baseband filtered OQPSK modulation. Subsections 3.2.2.3.1 and 3.2.2.3.2 address the aforementioned Butterworth and SRRC filters. Subsection 3.2.2.3.3.1 provides the characteristics of a Bessel filter which was not specifically recommended but is an example of other filter types which can meet the requirements of the SFCG mask and has good performance.

The Butterworth and Bessel filters are implemented as Infinite Impulse Response (IIR) filters, while the SRRC filter is implemented as a transversal Finite Impulse Response (FIR) filter. The implementation fidelity of these filters depends on the length of the filter, the sampling rate, and the amplitude quantization. The characteristics and design details of these filters is well documented in reference [6] and other textbooks.

3.2.2.3.1   Baseband Filtered OQPSK with a Butterworth Filter

This subsection describes the 6-pole BT_s = 0.5 Butterworth lowpass filter which is one of the filter types specifically recommended by the CCSDS for baseband filtered OQPSK. The magnitude and phase response of the filter are plotted in figure 3-23. The simulated power spectral density for both the I/Q and PM implementations of baseband filtered OQPSK with the Butterworth filter are presented in figure 3-24. The PSD is measured at the output of a saturated power amplifier to demonstrate the ability of the spacecraft using this modulation to meet the requirements of the SFCG emissions mask. The characteristics of the power amplifier are provided in annex B.
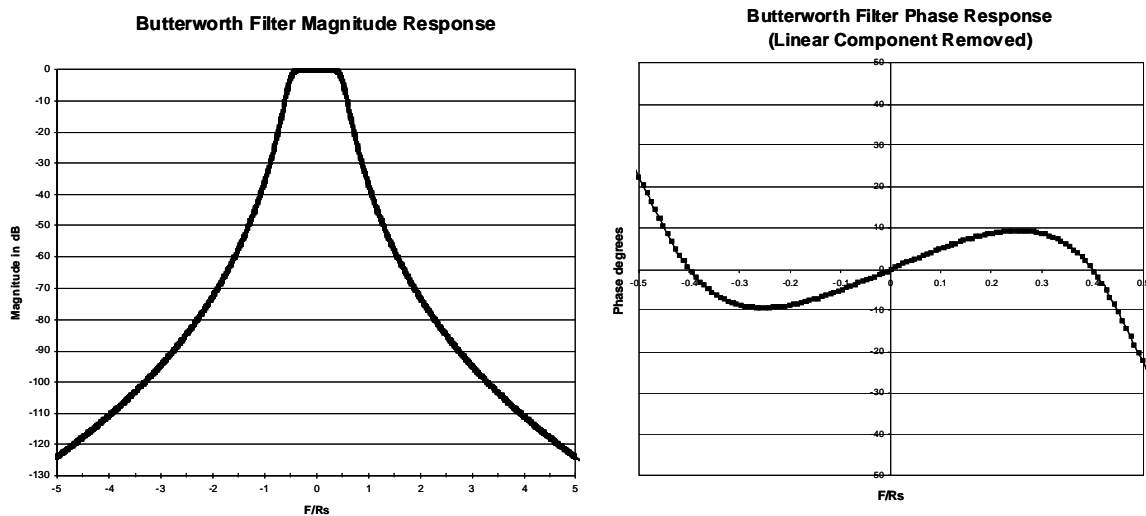
Figure 3-23: Butterworth Filter Magnitude and Phase Response
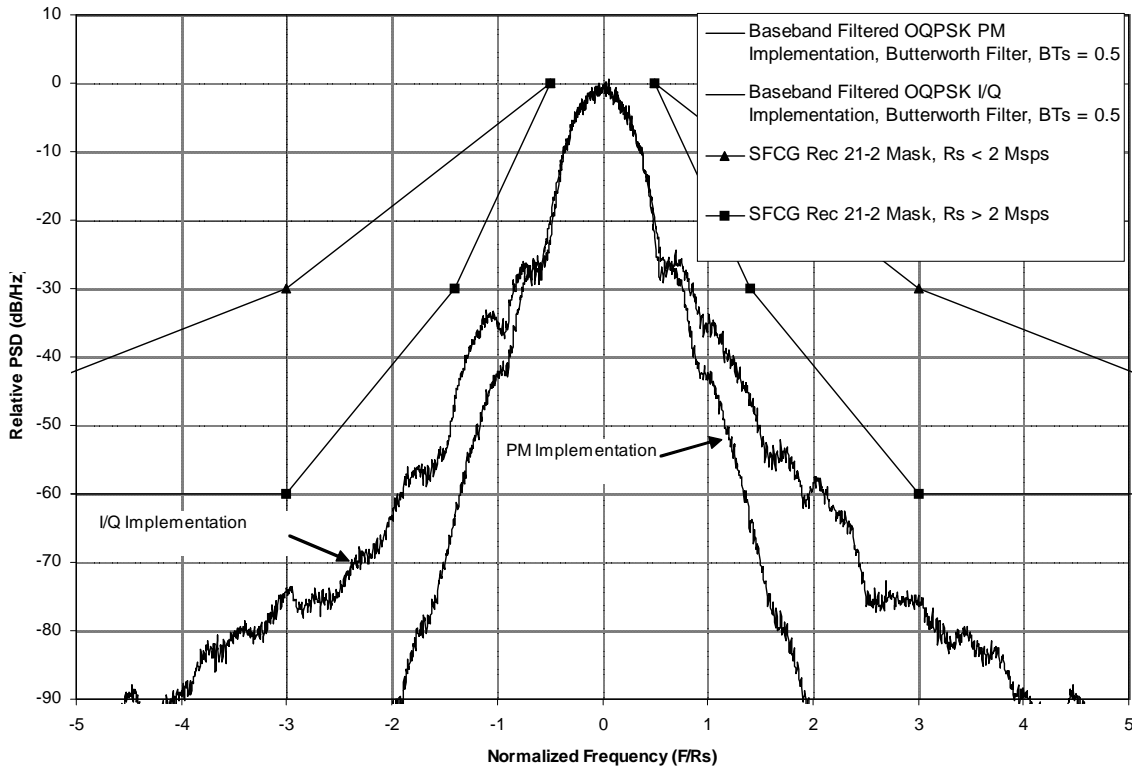
Figure 3-24: PSD for I/Q and PM Implementations of Baseband Filtered OQPSK with the Recommended Butterworth Filter

3.2.2.3.2   SRRC Filtered Offset-QPSK

Two variants of SRRC Offset-QPSK are described below. Square root raised cosine baseband filtered OQPSK can be formed by filtering rectangular NRZ pulses with a SRRC filter, similar to the Butterworth filtered OQPSK described in 3.2.2.3.1. A different form of SRRC OQPSK is created by using the impulse response of the SRRC filter as the signaling pulse shape. This type of SRRC OQPSK, described in 3.2.2.3.2.2, satisfies the Nyquist criterion for ISI-free signaling and is referred to as Nyquist pulse-shaped SRRC OQPSK in this Green Book to differentiate it from SRRC filtering of rectangular pulses.

3.2.2.3.2.1   Baseband Filtered OQPSK with a Square Root Raised Cosine Filter

This subsection describes the SRRC filter (α = 0.5) which is one of the filter types specifically recommended for baseband filtered OQPSK. The magnitude and phase response of the filter are plotted in figure 3-25. The simulated power spectral density for both the I/Q and PM implementations of baseband filtered OQPSK with the SRRC filter are presented in figure 3-26. The PSD is measured at the output of a saturated power amplifier to demonstrate the ability of the spacecraft using this modulation to meet the requirements of the SFCG emissions mask. The AM/AM and AM/PM characteristics of the power amplifier are provided in annex B.

Figure 3-25: Magnitude and Phase Response of SRRC (α = 0.5) Filter
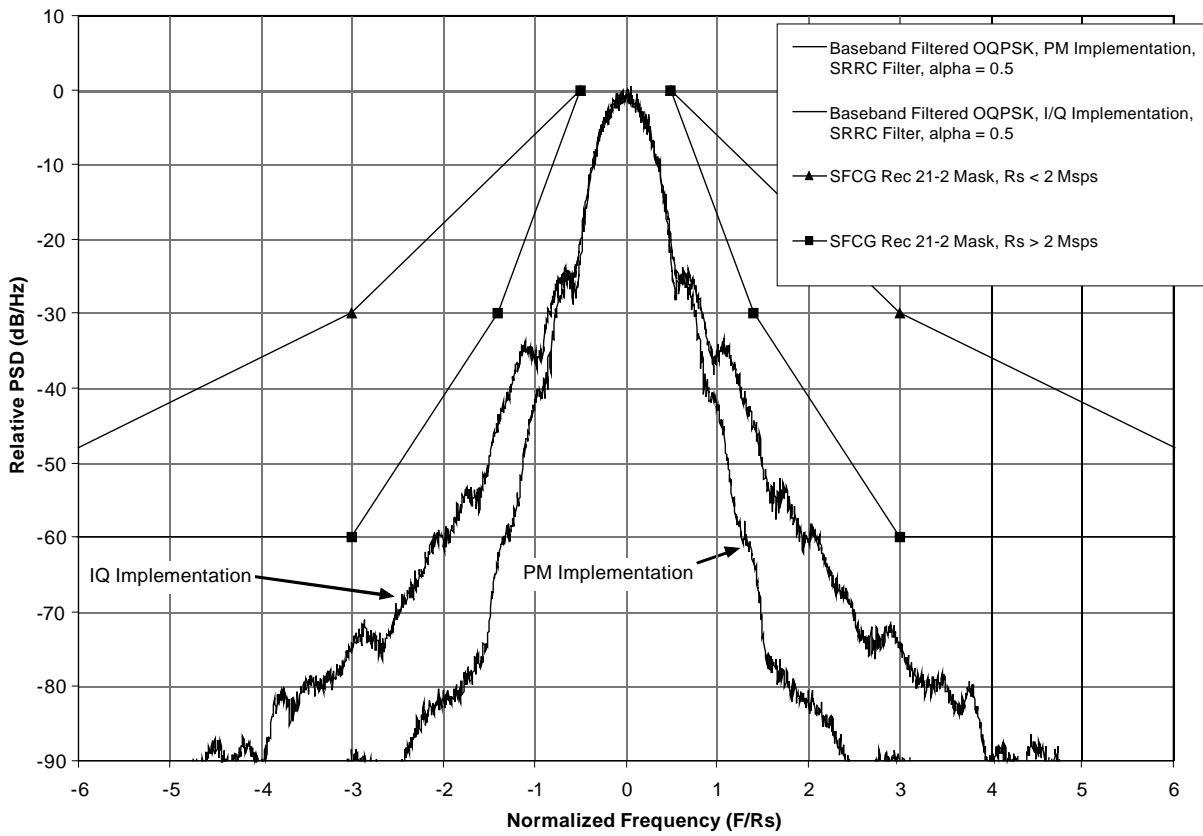
Figure 3-26: PSD for I/Q and PM Implementations of Baseband Filtered OQPSK with the Recommended SRRC Filter

3.2.2.3.2.2 Nyquist Pulse-Shaped SRRC OQPSK

A different form of SRRC OQPSK is created using the impulse response of the SRRC filter as the modulation pulse shape rather than SRRC filtering of NRZ pulses. With a matched filter receiver, this type of SRRC OQPSK fulfills the Nyquist criterion for ISI-free signaling. This means that in a linear channel with no timing errors, sampling points spaced T_{ChS} seconds apart at the output of the matched filter have no intersymbol interference. However, with distortion due to non-linear amplification, the Nyquist criterion is no longer satisfied and some ISI will occur.

Mathematically, Nyquist pulse-shaped SRRC OQPSK is defined as follows:

$$s(t) = d_I(t) * h(t)\sin(\omega_c t + \varphi_0) + d_Q\left(t - \frac{T_{Chs}}{2}\right) * h(t)\cos(\omega_c t + \varphi_0)$$

where * denotes convolution and h(t) is the SRRC filter impulse response defined by:

$$h(t) = \frac{4\alpha}{\pi\sqrt{T_{ChS}}} \frac{\cos\left(\frac{(1+\alpha)\pi t}{T_{ChS}}\right) + \frac{T_{ChS}}{4\alpha t}\sin\left(\frac{(1-\alpha)\pi t}{T_{ChS}}\right)}{1 - \left(4\alpha t / T_{ChS}\right)^2}$$

and $d_I(t)$ and $d_Q(t)$ are the I and Q impulse streams defined by:

$$d_I(t) = \sum_k I_k \delta(t - kT_{ChS})$$

$$d_Q(t) = \sum_k Q_k \delta(t - kT_{ChS})$$

where $\delta(t)$ is the Dirac delta function, and I_k and Q_k are the inphase and quadrature phase data symbol streams. The roll-off factor α determines the frequency from the filter passband to the stopband is very abrupt while the filter impulse response is spread out in time. For large values of α, the filter roll-off is more gradual while conversely the impulse response is more concentrated in time. The case of $\alpha=0$ corresponds to an instantaneous transition from the filter passband to the stopband at the cutoff frequency, often called a 'brickwall' filter.

Figure 3-27 shows a block diagram of a Nyquist pulse-shaped SRRC OQPSK modulator based on the theoretical equations above. With digital implementation, the SRRC filter is typically windowed since the impulse response is theoretically infinite in time. The FIR coefficients of the windowed SRRC filter can then be stored in ROM lookup tables.

Transmitter hardware distortions including amplifier nonlinearities and windowing create intersymbol interference and cause spectral regrowth for the Nyquist SRRC OQPSK signal. For smaller values of α, the effects of signal distortion will be more severe. Figure 3-28 shows the simulated Nyquist SRRC OQPSK ($\alpha=0.5$) spectrum at the output of the saturated (defined as 0 dB output back-off) SSPA whose characteristics are given in annex B.
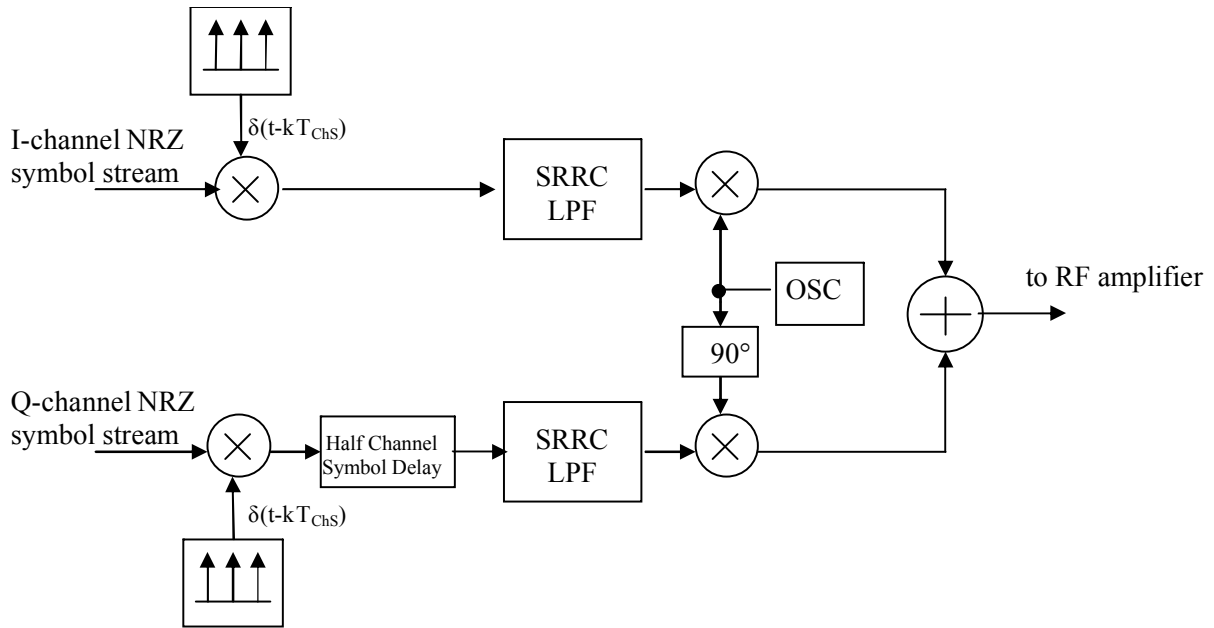
Figure 3-27: Nyquist Pulse-Shaped SRRC OQPSK Modulator Based on Theoretical Equation
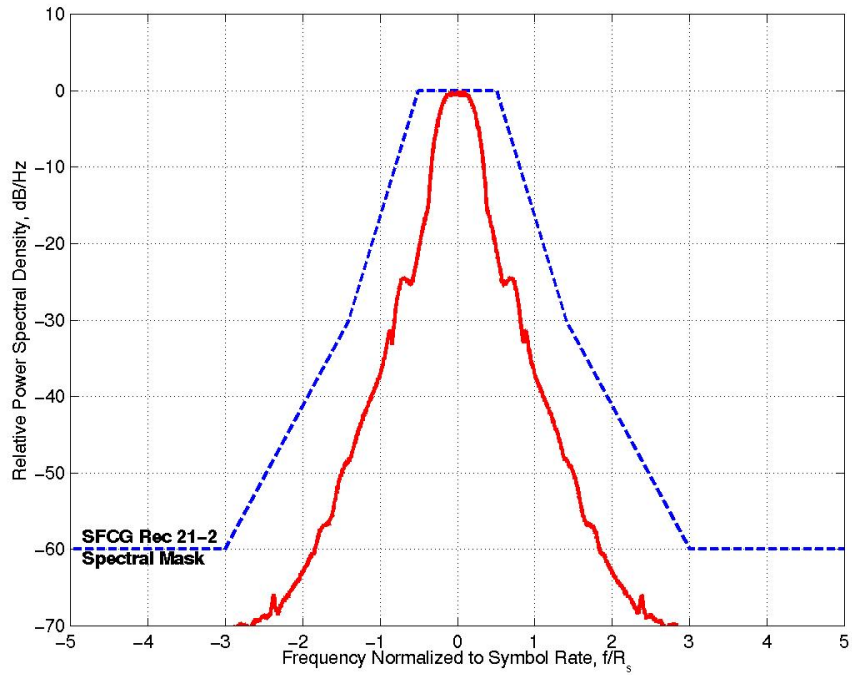
Figure 3-28: Simulated Spectrum of Nyquist Pulse-Shaped SRRC (α=0.5) OQPSK at Output of Saturated SSPA

3.2.2.3.3   Baseband Filtered OQPSK with Other Filter Types

As indicated above, Butterworth and/or SRRC filters are not necessarily optimum for use in baseband filtered OQPSK systems.   While it would be impossible to document the performance of all possible filters, the performance of Bessel-filtered OQPSK is addressed in the following subsection as an example.

3.2.2.3.3.1   Baseband Filtered OQPSK with Bessel Filter

This subsection describes a 6th order $BT_s = 0.5$ Bessel filter.   The magnitude and phase response of the filter are plotted in figure 3-29.   The simulated power spectral density for both the I/Q and PM implementations of baseband filtered OQPSK with the Bessel filter are presented in figure 3-30.   The PSD is measured at the output of a saturated power amplifier to demonstrate the ability of the spacecraft using this modulation to meet the requirements of the SFCG emissions mask.   The characteristics of the power amplifier are provided in annex B.
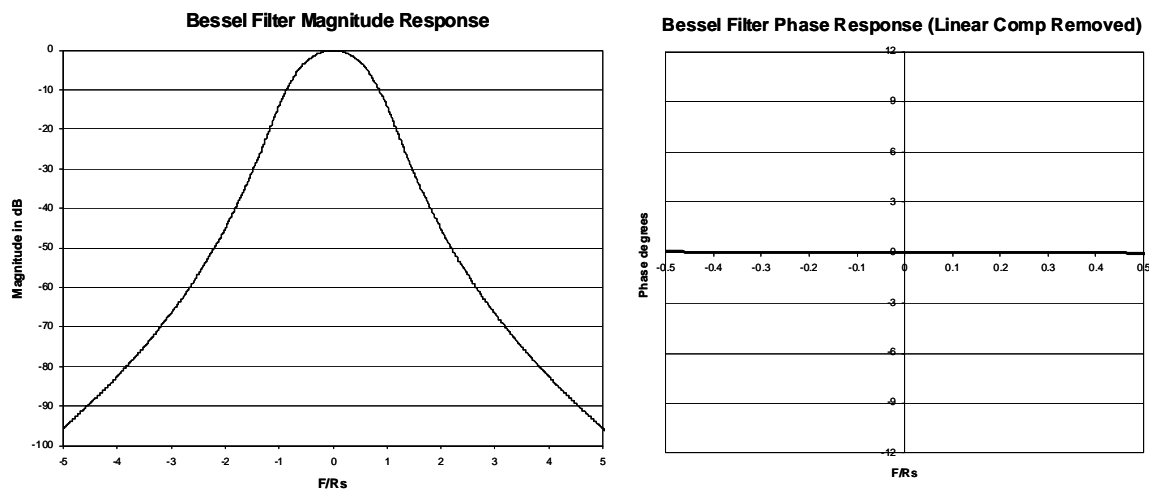
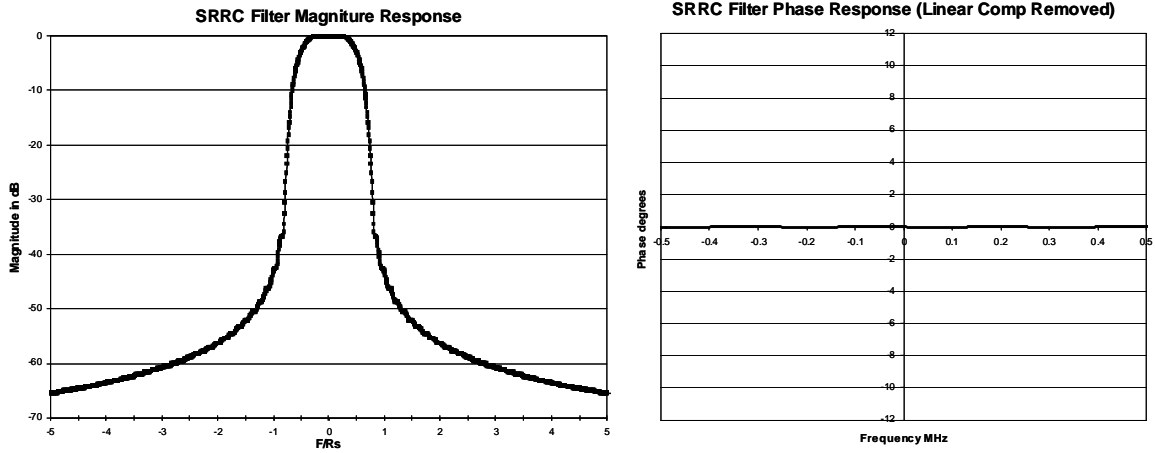**Figure 3-29:   Magnitude and Phase Response of 6th Order $BT_s = 0.5$ Bessel Filter**
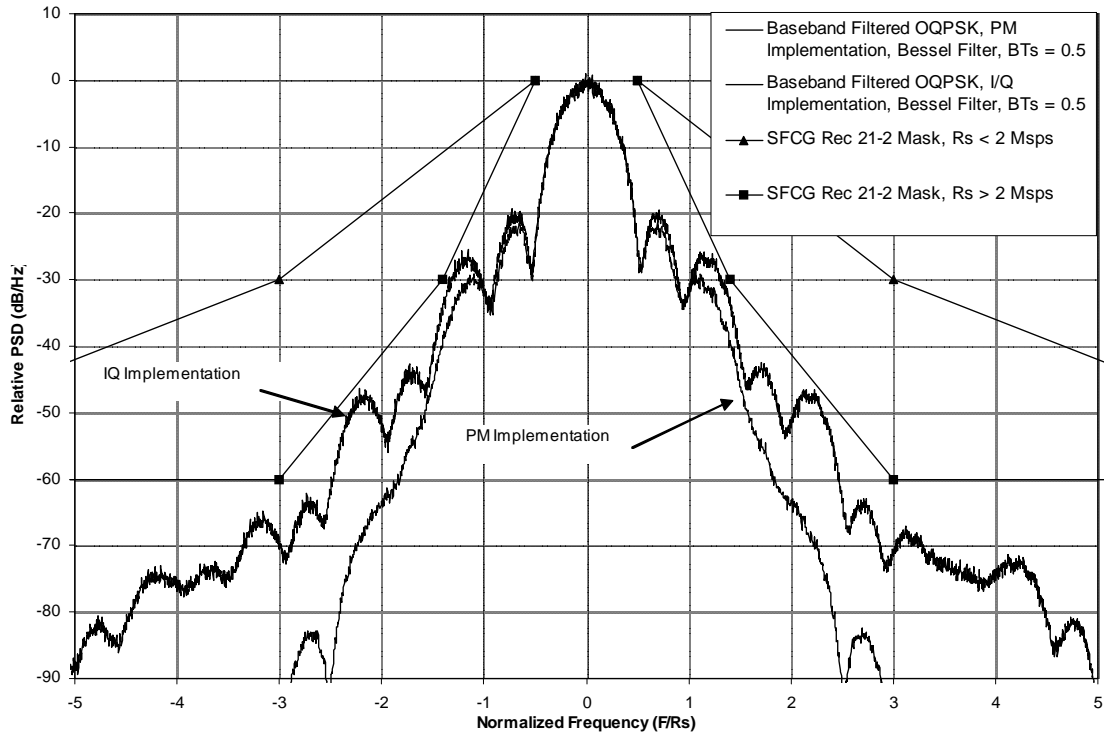
Figure 3-30: PSD for I/Q and PM Implementations of Baseband Filtered OQPSK with a 6th Order BT_s = 0.5 Bessel Filter

3.3 4D 8PSK TRELLIS-CODED MODULATION

This subsection specifies the coding and mapping techniques integral to a highly efficient multidimensional trellis coded modulation for use in bandwidth-constrained communications between remote satellites and Earth stations. Efficiency in this context refers both to bandwidth efficiency (in bits/s/Hz and bits/channel-symbol) for a given information quantity, and power efficiency. The basic principle and requirements for implementation of multidimensional 8PSK TCM is given in the following subsections.

3.3.1 INTRODUCTION

The L-dimensional MPSK-TCM (LD-MPSK-TCM) belongs to a family of modulations first introduced by G. Ungerboeck (reference [7]) and improved by S. Pietrobon (reference [8]) with the introduction of the multidimensional techniques.

The MPSK-TCM are based on MPSK modulations with the use of convolutional coding to introduce 'authorized sequences' between signal points linked by the trellis of the code. Single constellation MPSK modulations may also be referred to as 'bidimensional' in reference to the representation of the MPSK constellation points in a signal space defined by orthogonal I and Q vectors. In any case, the application of this procedure to several parallel constellations of the same size is referred to as L-dimensional TCM, denoted LD-MPSK-

TCM (with L > 1 and M ≥ 8). The trellis is constructed to maximize the minimum Euclidian distance between different paths originating and merging to the same state. The construction of the optimum trellis code and partitioning for the M points in the constellation is based on heuristic rules proposed in references [7] and [8].

With 4D-8PSK-TCM, the combination of convolutional coding, multiphase modulation and multidimensional techniques offers a substantial power gain together with bandwidth conservation or reduction, in comparison to their separate utilization as it is done frequently with binary or quaternary modulations (i.e., sequential implementation of convolutional coding). The result is an improvement of the performances in terms of BER versus signal to noise ratio for the same or better bandwidth efficiency, compared with the uncoded OQPSK or QPSK modulations.

Example: Assuming the bit rate R_b of input data equal to 100 Mbps, the 4D-8PSK-TCM channel symbol rate is 50 Ms/s for 2 bits/channel-symbol or 40 Ms/s for 2.5 bits/channel-symbol.

3.3.2   4D-8PSK-TCM CODER

The 4D-8PSK trellis-coded modulator consists of a serial-to-parallel converter, a differential coder, a trellis encoder (convolutional coder), a constellation mapper, and an 8PSK modulator (see figure 3-31). In this figure, wi (with index i = 1, … , m) represent the uncoded bits and xj (with index j = 0, … , m) are the coded bits. The trellis encoder is based on a 64-state systematic convolutional coder and can be considered as the inner code if an outer block code is introduced. Carrier phase ambiguity is resolved by the use of a differential coder located prior to the trellis encoder. Spectral efficiencies of 2, 2.25, 2.5, and 2.75 bits/channel-symbol are achieved with four possible architectures of the constellation mapper. The output switch addresses successively one of the four symbols ($Z^{(0)} - Z^{(3)}$) from the constellation mapper to the 8PSK modulator.

The present standard is based on the use of a 4D-8PSK-TCM characterized by the following parameters:

- size of the constellation: M=8 phase states (8PSK);

- number of signal set constituents: L=4 (shown as $Z^{(0)}$ … $Z^{(3)}$ in figure 3-31);

- number of states for the trellis encoder: 64;

- rate of the convolutional coder used for the construction of the trellis: R=3/4;

- rate of the modulation: R_m=m/(m+1) selectable to 8/9, 9/10, 10/11, or 11/12;

- efficiency of the modulation:

  - Reff=2 bits per channel-symbol (for Rm=8/9);

  - Reff=2.25 bits per channel-symbol (for Rm=9/10);

- Reff=2.5 bits per channel-symbol (for Rm=10/11);

- Reff=2.75 bits per channel-symbol (for Rm=11/12).
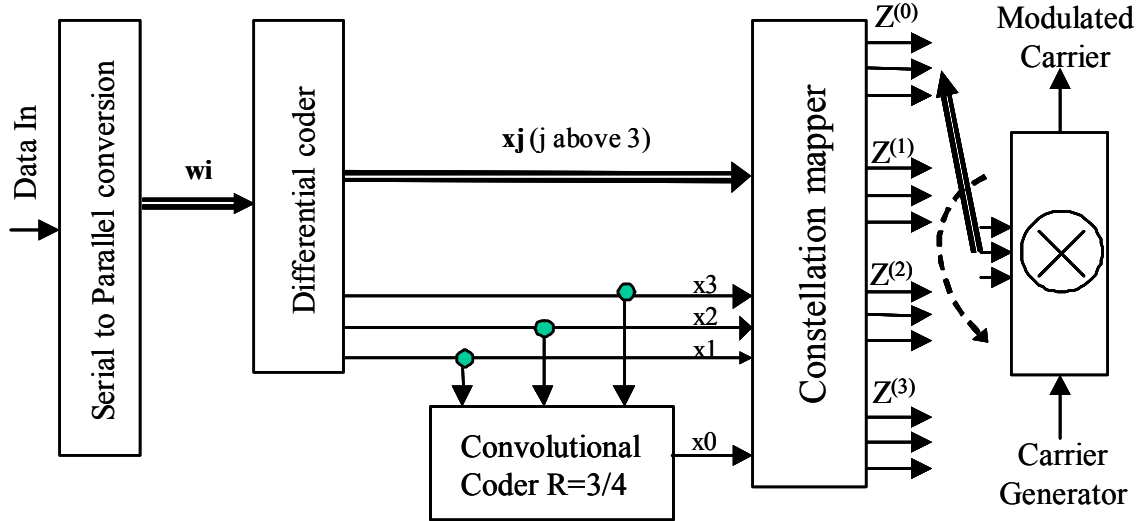
Figure 3-31: Structure of the 4D 8PSK-TCM Coder/Mapper

3.3.2.1 Differential Coder

The differential coder depicted in figure 3-32 is used to eliminate phase ambiguity on carrier synchronization for each modulation efficiency. Table 3-1 gives the bit reference at input and output of the differential coder in each case.

Table 3-1: Bit Mapping for Differential Coder

Efficiencies in bits /channel-symbol							
2		2.25		2.5		2.75	
bit IN	bit OUT	bit IN	bit OUT	bit IN	bit OUT	bit IN	bit OUT
w1	x1	w2	x2	w3	x3	w4	x4
w5	x5	w6	x6	w7	x7	w8	x8
w8	x8	w9	x9	w10	x10	w11	x11

An example of differential encoder connections is given in figure 3-32 for the 2 bits/channel-symbol case. The structure of the modulo 8 adder is also shown; it is applicable to both the coder mapper and differential coder.

$c_0 = a_0 \oplus b_0$ with carry r_0

$c_1 = a_1 \oplus b_1 \oplus r_0$ with carry r_1

$c_2 = a_2 \oplus b_2 \oplus r_1$

$r_0 = a_0.b_0$

$r_1 = (a_1.b_1) + (a_1.r_0) + (b_1.r_0)$

where . corresponds to a logical AND, and + to a logical OR
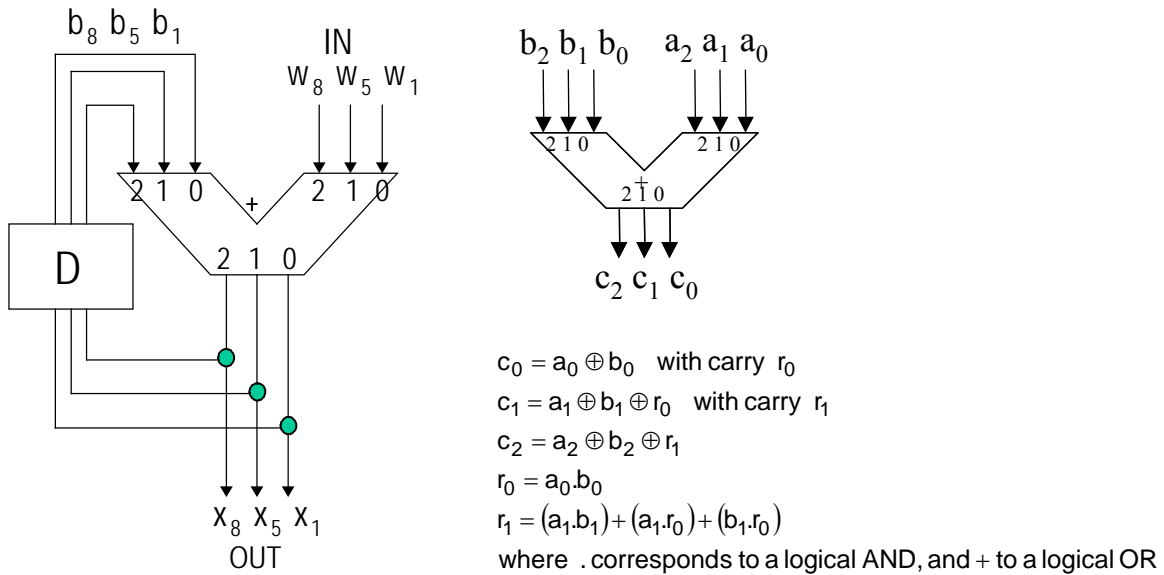
Figure 3-32: Differential Coder and Modulo-8 Adder Principle

3.3.2.2 Convolutional Coder

The convolutional coder used to implement the trellis is based on the work described in reference [8] and is depicted in figure 3-33. This code corresponds to one of the 'best' codes for phase transparency.

The systematic coder is implemented with the following characteristics:

- number of states: 64 states;

- constraint length: K = 7;

- rate = 3/4.

The convolutional encoder is specified by the following polynomial in octal: $h^3 = 050$, $h^2 = 024$, $h^1 = 006$, $h^0 = 103$. Figure 3-33 shows the recommended convolutional encoder. The shift registers of the encoder are clocked at the rate of $R_{ChS}/4$.
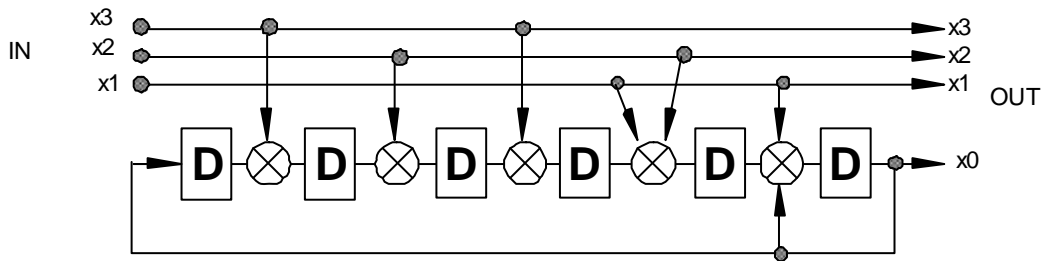
Figure 3-33: Convolutional Coder Recommended for High Data Rates

The number of coded bits is the same for the four modulation efficiencies (i.e., the same structure is used for 2, 2.25, 2.5, and 2.75 bits/channel-symbol), only the number of uncoded bits is changed. The advantage of this coder is its optimized performance and the reduced internal rate which is equal to 1/8, 1/9, 1/10, or 1/11 of the information rate.

3.3.2.3   Constellation Mapper for 4D-8PSK-TCM

The constellation mapper principles are given in figures 3-34 to 3-37 for the four possible efficiencies of this modulation (i.e., 2 bits/channel-symbol, 2.25 bits/channel-symbol, 2.5 bits/channel-symbol and 2.75 bits/channel-symbol). These mappers implement the straightforward logical mapping described in the equations below. The correspondence between the signals $Z^{(i)}$ at the input of the modular and the 8PSK phase states of the constellations follows a natural mapping (i.e., 0, 1, 2 …, 7).

If $Z^{(i)}$ represents the signals (three lines) at the input of the modulator with $Z^{(0)}$ being the signal set of the first constellation and $Z^{(3)}$ being the signal set of the fourth constellation, the signal set $Z^{(i)}$ is represented by the following equation. This representation shows that the bits which are common to each vector set (shown in the first part of right-hand side of each equation) are sensitive to a phase rotation of $\pi/4$ and will be differentially encoded (see 3.3.2.1).

(i) <u>Equation for 2 bits/channel-symbol efficiency</u>

$$\begin{bmatrix} Z^{(0)} \\ Z^{(1)} \\ Z^{(2)} \\ Z^{(3)} \end{bmatrix} = \left[\left(4x^{(8)} + 2x^{(5)} + x^{(1)} \right) \begin{pmatrix} 1 \\ 1 \\ 1 \\ 1 \end{pmatrix} + 4 \begin{pmatrix} 0 \\ x^{(7)} \\ x^{(6)} \\ x^{(7)} + x^{(6)} + x^{(4)} \end{pmatrix} + 2 \begin{pmatrix} 0 \\ x^{(3)} \\ x^{(2)} \\ x^{(3)} + x^{(2)} + x^{(0)} \end{pmatrix} \right] \bmod 8$$
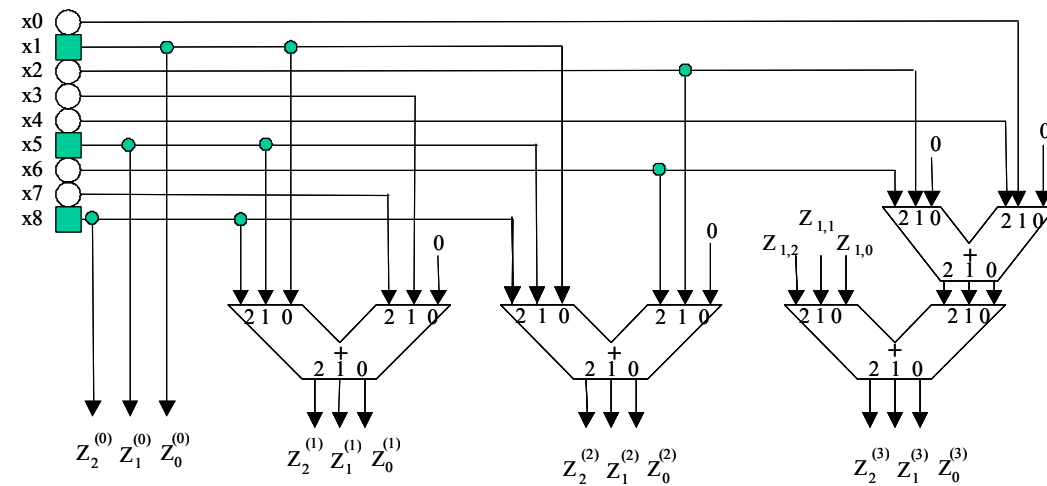
$\square$ = line connected to differential coder

$\bigcirc$ = line connected to serial-to-parallel converter or convolutional coder

Figure 3-34: Constellation Mapper for 2 Bits/Channel-Symbol

(ii) <u>Equation for 2.25 bits/channel-symbol efficiency</u>

$$\begin{bmatrix} Z^{(0)} \\ Z^{(1)} \\ Z^{(2)} \\ Z^{(3)} \end{bmatrix} = \left[\left(4x^{(9)} + 2x^{(6)} + x^{(2)}\right)\begin{pmatrix} 1 \\ 1 \\ 1 \\ 1 \end{pmatrix} + 4\begin{pmatrix} 0 \\ x^{(8)} \\ x^{(7)} \\ x^{(8)} + x^{(7)} + x^{(5)} \end{pmatrix} + 2\begin{pmatrix} 0 \\ x^{(4)} \\ x^{(3)} \\ x^{(4)} + x^{(3)} + x^{(1)} \end{pmatrix} + \begin{pmatrix} 0 \\ x^{(0)} \\ 0 \\ x^{(0)} \end{pmatrix} \right] \bmod 8$$
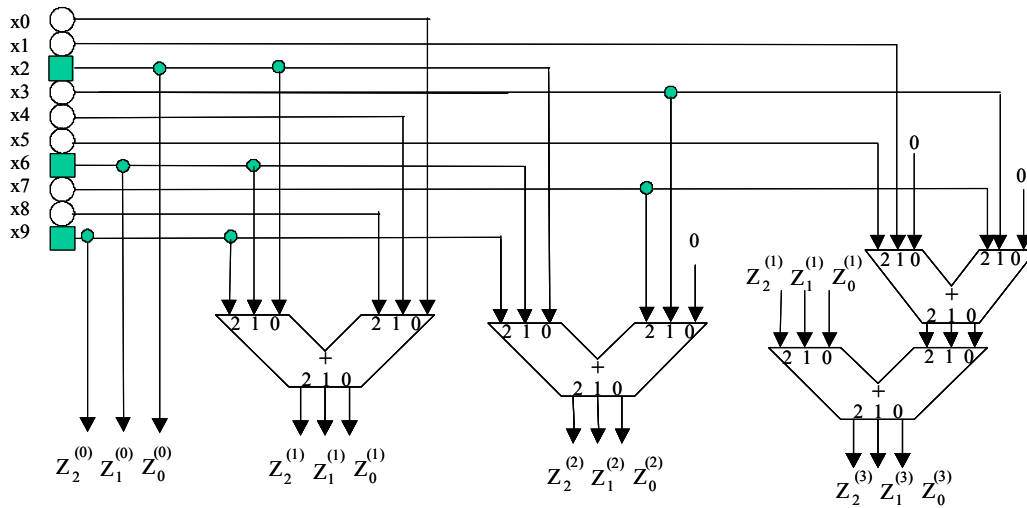
$\blacksquare$ = line connected to differential coder

$\bigcirc$ = line connected to serial-to-parallel converter or convolutional coder

Figure 3-35: Constellation Mapper for 2.25 Bits/Channel-Symbol

(iii) <u>Equation for 2.5 bits/channel-symbol efficiency</u>

$$
\begin{bmatrix} Z^{(0)} \\ Z^{(1)} \\ Z^{(2)} \\ Z^{(3)} \end{bmatrix} = \left[\left(4x^{(10)} + 2x^{(7)} + x^{(3)} \right) \begin{pmatrix} 1 \\ 1 \\ 1 \\ 1 \end{pmatrix} + 4 \begin{pmatrix} 0 \\ x^{(9)} \\ x^{(8)} \\ x^{(9)} + x^{(8)} + x^{(6)} \end{pmatrix} + 2 \begin{pmatrix} 0 \\ x^{(5)} \\ x^{(4)} \\ x^{(5)} + x^{(4)} + x^{(2)} \end{pmatrix} + \begin{pmatrix} 0 \\ x^{(1)} \\ x^{(0)} \\ x^{(1)} + x^{(0)} \end{pmatrix} \right] \mod 8
$$
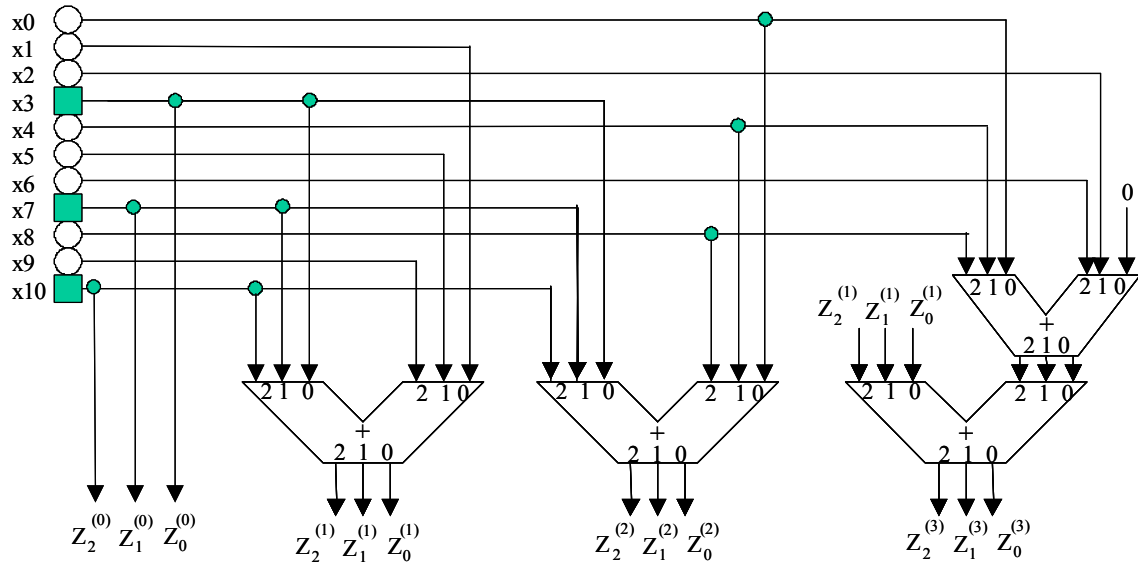
$\blacksquare$ = line connected to differential coder

$\bigcirc$ = line connected to serial-to-parallel converter or convolutional coder

Figure 3-36: Constellation Mapper for 2.5 Bits/Channel-Symbol

(iv) Equation for 2.75 bits/channel-symbol efficiency

$$
\begin{bmatrix} Z^{(0)} \\ Z^{(1)} \\ Z^{(2)} \\ Z^{(3)} \end{bmatrix} = \left[\left(4x^{(11)} + 2x^{(8)} + x^{(4)} \right) \begin{pmatrix} 1 \\ 1 \\ 1 \\ 1 \end{pmatrix} + 4 \begin{pmatrix} 0 \\ x^{(10)} \\ x^{(9)} \\ x^{(10)} + x^{(9)} + x^{(7)} \end{pmatrix} + 2 \begin{pmatrix} 0 \\ x^{(6)} \\ x^{(5)} \\ x^{(6)} + x^{(5)} + x^{(3)} \end{pmatrix} + \begin{pmatrix} 0 \\ x^{(2)} \\ x^{(1)} \\ x^{(2)} + x^{(1)} + x^{(0)} \end{pmatrix} \right] \mod 8
$$
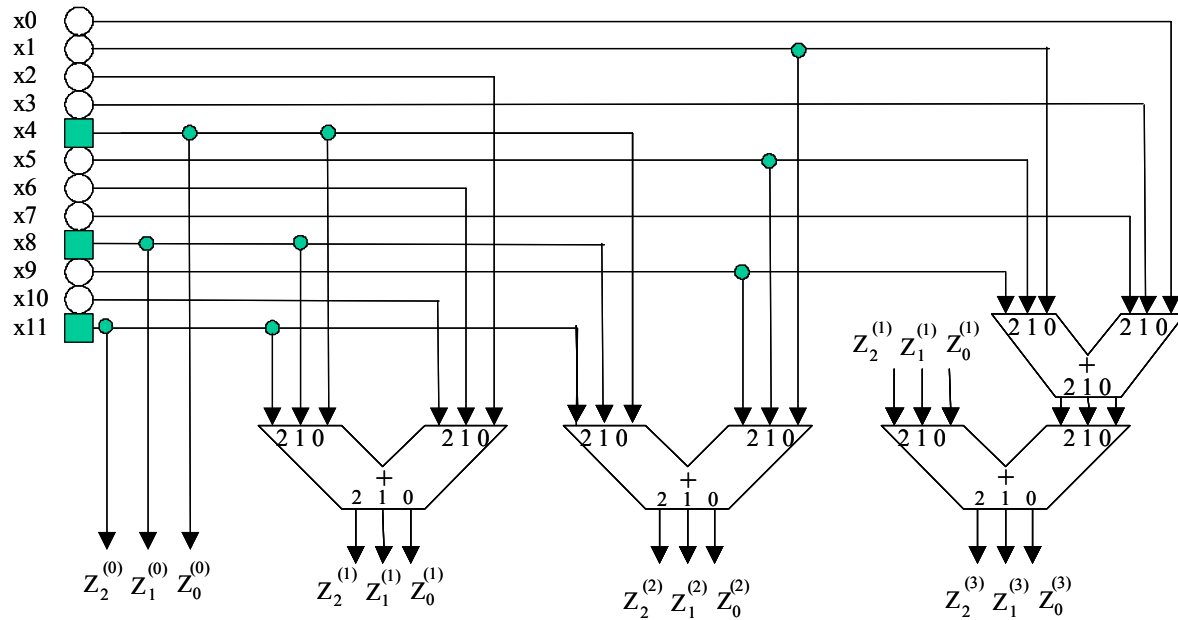
$\blacksquare$ = line connected to differential coder

$\bigcirc$ = line connected to serial to parallel converter or convolutional coder

Figure 3-37: Constellation Mapper for 2.75 Bits/Channel-Symbol

3.3.2.4 Coder/Mapper Implementation at 2, 2.25, 2.5 and 2.75 Bits/Channel-Symbol Efficiency

The principle of the coder-mapper for 2, 2.25, 2.5, and 2.75 bits/channel-symbol efficiency is given in figures 3-38 through 3-41.
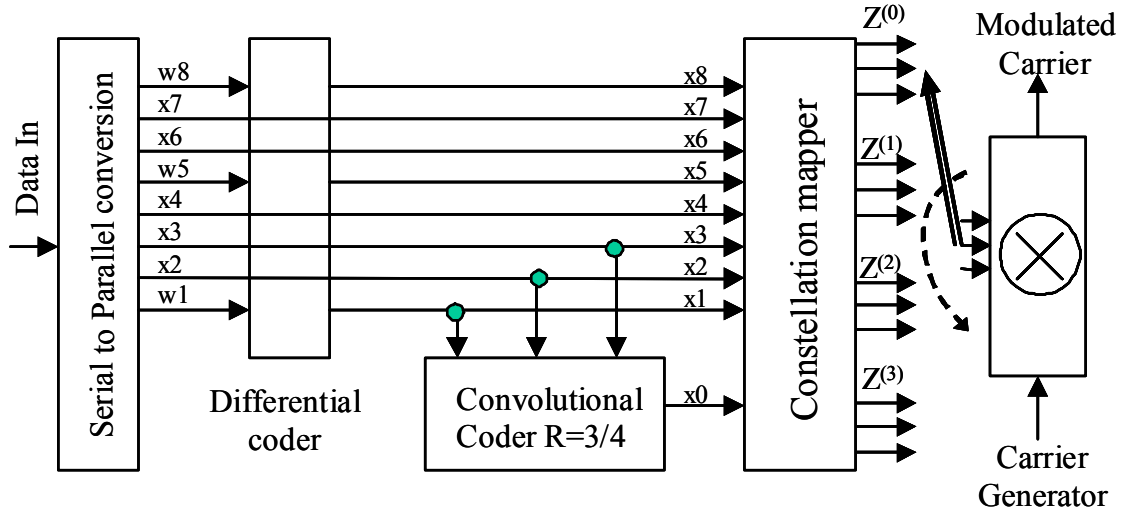
Figure 3-38: Coder and Mapper Implementation for 2 Bits/Channel-Symbol Efficiency
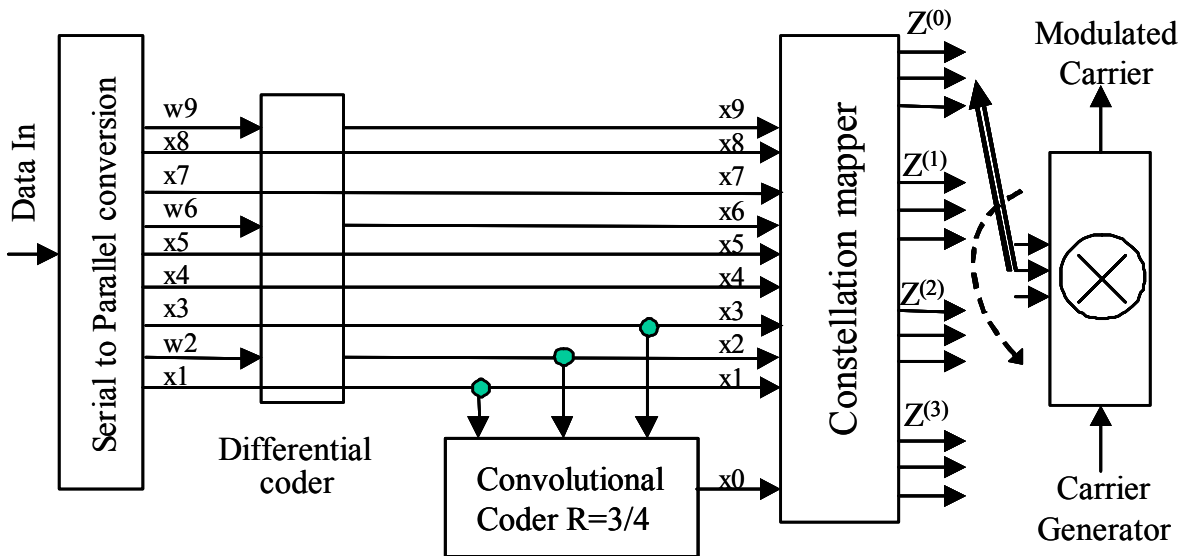
Figure 3-39: Coder and Mapper Implementation at 2.25 Bits/Channel-Symbol Efficiency
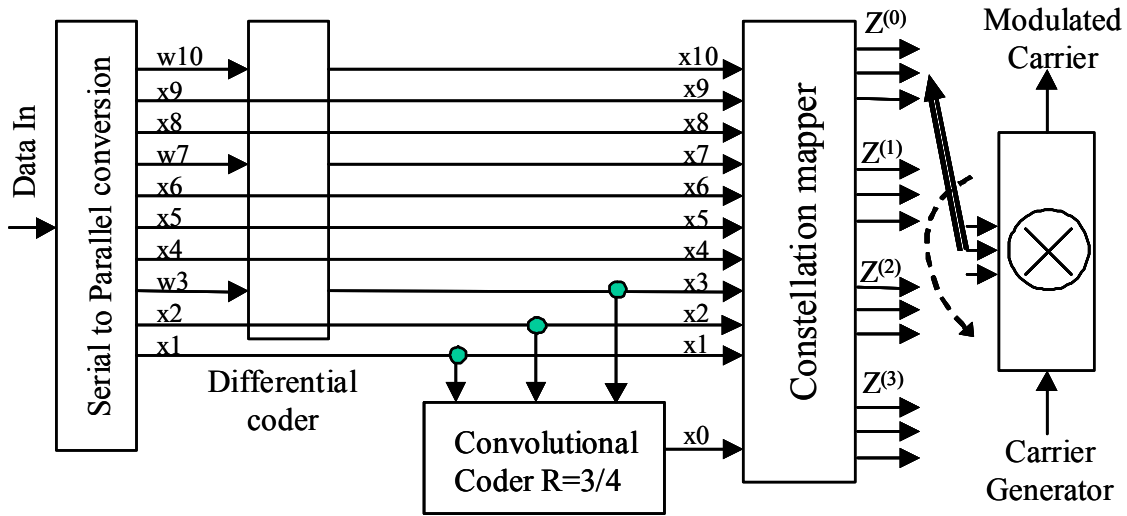
Figure 3-40: Coder and Mapper Implementation at 2.5 Bits/Channel-Symbol Efficiency
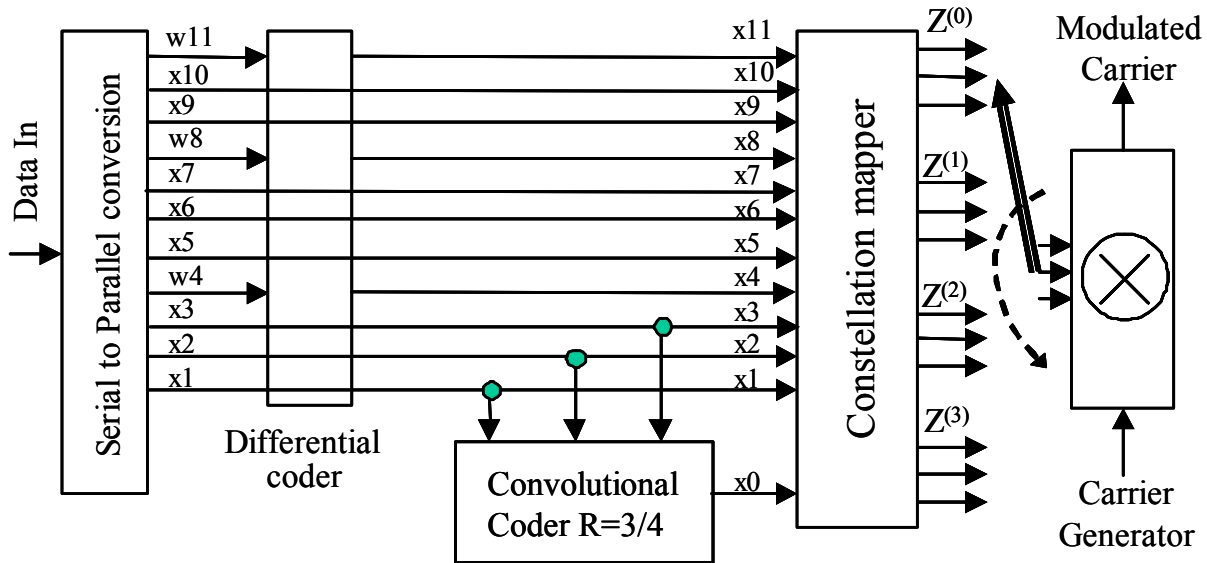
Figure 3-41: Coder and Mapper Implementation at 2.75 Bits/Channel-Symbol Efficiency

3.3.3 4D-8PSK-TCM PHASE NOISE RECOMMENDATION

It is recommended that the phase noise for all the oscillators of the 4D-8PSK-TCM communication chain be limited according to the mask given in figure 3-42 for channel symbol rates from 1 Ms/s up to 100 Ms/s. The figure shows the double-sided phase noise mask 2L(f) in dBc/Hz versus frequency in Hz.
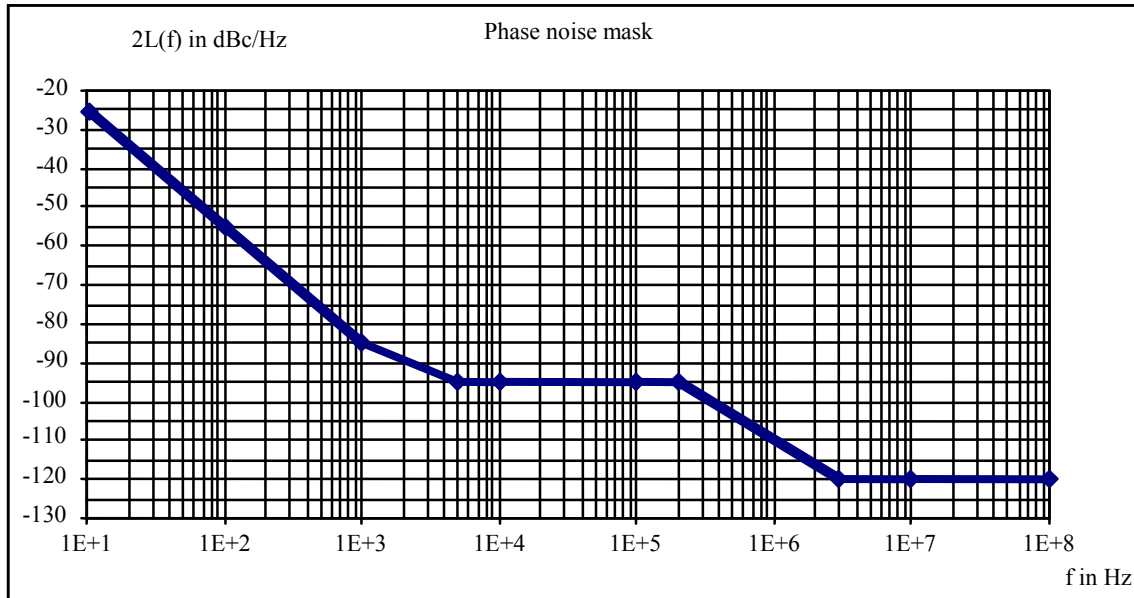
Figure 3-42: 4D-8PSK-TCM Phase Noise Mask Recommendation

3.3.4 CHANNEL FILTERING

Channel filtering is to be obtained by one of the following methods:

− Square root raised cosine (SRRC) baseband shaping filter located prior to the modulator, with a channel roll-off factor α of 0.35 or 0.5. This waveform shaping is used in conjunction with a linear modulator and power amplifier.

− Post-amplifier shaping using a filter located at the output of a non-linear power amplifier. In this case, post-amplifier filtering of the NRZ 8-PSK signal is used in conjunction with a non-linear phase modulator or power amplifier.

In both cases, the pre-detection filter (matched filter) in the receiver shall be a SRRC filter with a roll-off factor α of 0.35 or 0.5.

3.3.4.1 Baseband SRRC Shaping

Baseband SRRC shaping should be used when the power amplifier is operated in a linear region, when the symbol rate to center frequency ratio is low, or when there is amplifier linearization.

The normalized transfer function of the SRRC filter, H(f), is given by:[6]

$$H(f) = \begin{cases} 1 & |f| < f_N(1-\alpha) \\ \sqrt{\dfrac{1}{2} + \dfrac{1}{2}\sin\left(\dfrac{\pi}{2f_N}\left[\dfrac{f_N - |f|}{\alpha}\right]\right)} & f_N(1-\alpha) \leq |f| \leq f_N(1+\alpha) \\ 0 & |f| > f_N(1+\alpha) \end{cases}$$

where $f_N = 1/(2T_{ChS}) = R_{ChS}/2$ is the Nyquist frequency, and α is the roll-off factor. The corresponding impulse response of the SRRC filter is given by:

$$h(t) = \frac{4\alpha}{\pi\sqrt{T_{ChS}}} \frac{\cos\left(\dfrac{(1+\alpha)\pi t}{T_{ChS}}\right) + \dfrac{T_{ChS}}{4\alpha t}\sin\left(\dfrac{(1-\alpha)\pi t}{T_{ChS}}\right)}{1 - \left(4\alpha t / T_{ChS}\right)^2}$$

The transmitter structure when using baseband SRRC shaping is shown in figure 3-43.
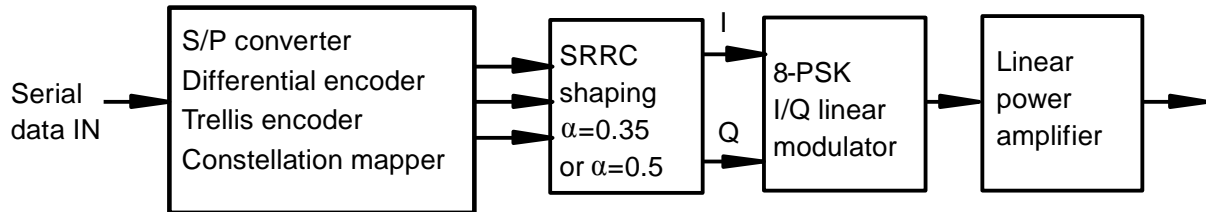
Figure 3-43: Transmit Structure for Baseband Square Root Raised Cosine Shaping

---

[6] The unnormalized value of H(f) can be obtained by multiplying its normalized value by $\sqrt{T_{ChS}}$.

Since SRRC shaping does not produce a constant envelope signal and causes some intersymbol interference when not matched with another SRRC filter, the phasor diagrams exhibit bowls around the phase points as shown in figure 3-44 (noise free conditions). For simplicity, phase transitions are not shown in the figure.
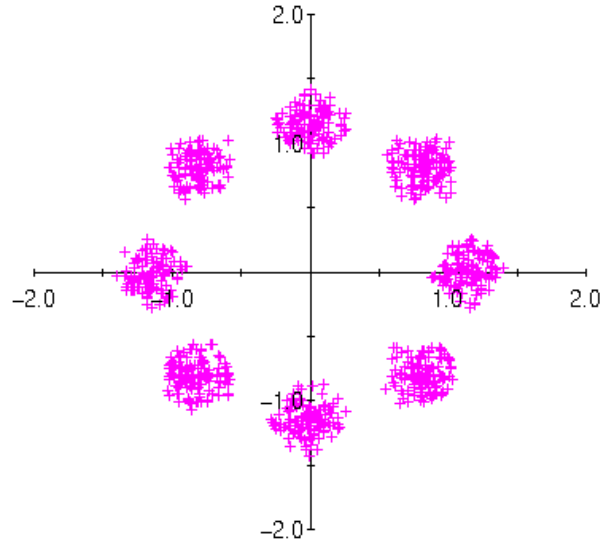
Figure 3-44: SRRC ($\alpha = 0.35$) Shaped 4D-8PSK-TCM Phasor Diagram

After SRRC matched filtering at the receiver, the resultant waveform consists of overlapping raised cosine (RC) pulse shapes. The eye diagram of the phase values between $-\pi$ to π is shown in figure 3-45 (plotted with 4-times oversampling). As the figure shows, good symbol synchronization is needed to avoid degradation due to ISI. The time axis is normalized by T_{ChS} with a $T_{ChS}/2$ offset so that the maximum eye opening is centered in the figure.
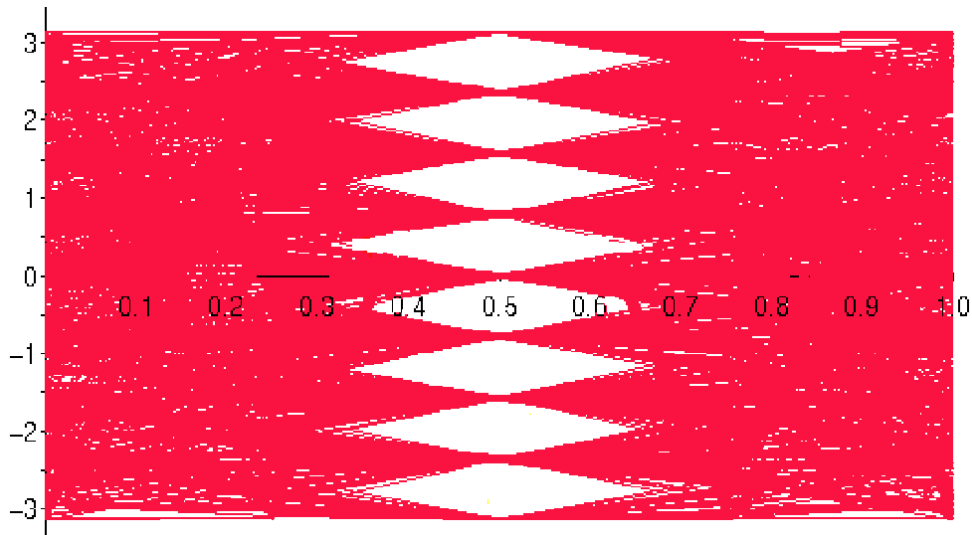
Figure 3-45: RC ($\alpha = 0.35$) Shaped 4D-8PSK-TCM Phase Eye Diagram at Output of Matched Filter

3.3.4.2 Post-Amplifier Shaping

Post-amplifier shaping should be used for non-linear amplifier conditions or when the ratio of the symbol rate to center frequency is high. The post-amplifier filtering should be obtained with a four pole/two zero RF elliptic filter characterized by the normalized transfer function given in the figure 3-46.

$10*\log (H^2(f))$
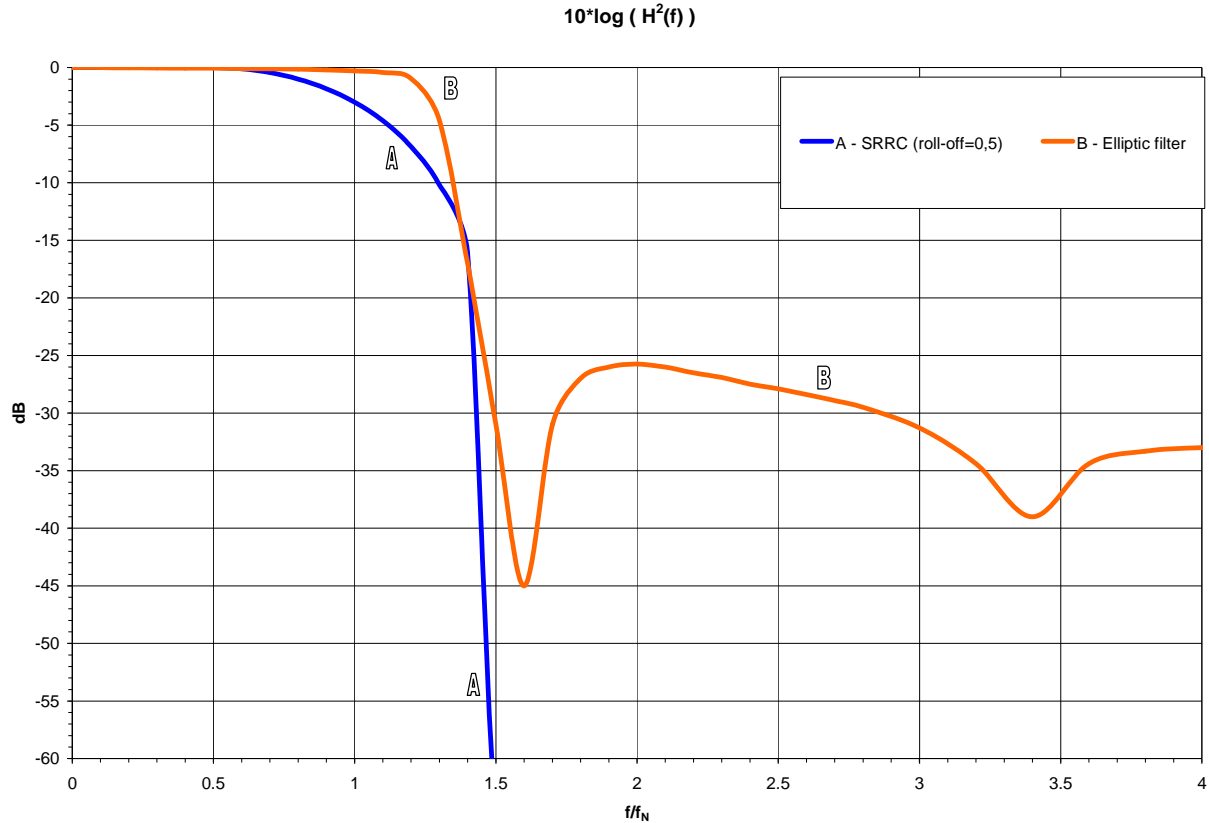
Figure 3-46: Transfer Function for 4 Poles/2 Zeros Elliptic Filter

The corresponding transmit structure when using post-amplifier shaping is shown in figure 3-47.
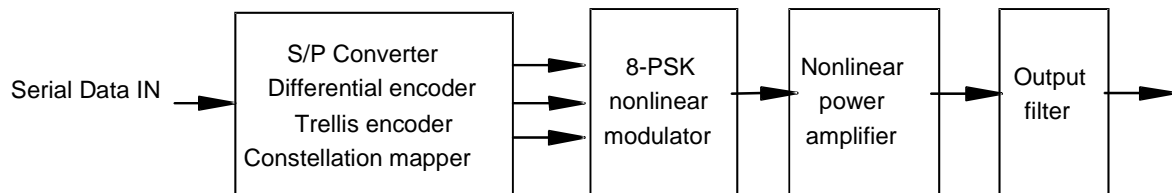
Figure 3-47: Transmit Structure for Post-Amplifier Shaping

4   SUMMARY

With more missions at high data rates demanding use of limited spectral resources for space-to-Earth telemetry, the SFCG issued Recommendations 21-2R2 and 23-1 to limit the spectral bandwidth of the Category A missions in the SRS and EESS bands, as well as of Category B missions. The CCSDS was commissioned by the SFCG to recommend bandwidth-efficient modulations which could meet the SFCG spectral masks and provide good end-to-end performance.

After extensive study and analysis, the CCSDS approved recommendations 401 (2.4.17A) B-1, 401 (2.14.17) B-1, 401 (2.4.18) B-1, and 401 (2.4.20B) B-1 addressing the use of bandwidth-efficient modulations for high data rate missions in the SRS and EESS frequency allocations.   Table 4-1 summarizes the CCSDS recommended bandwidth-efficient modulations and their respective frequency bands. A record of the CCSDS studies can be found in the CCSDS Yellow Book *Proceedings of the Bandwidth-Efficient Modulations Working Documents* (reference [1]).

This Green Book on bandwidth-efficient modulations supplements the three CCSDS recommendations on bandwidth-efficient modulations by providing technical descriptions of these modulations. The performance of these modulations is dependent on the many factors including channel coding, power amplifier nonlinearities, receiver type, channel characteristics, and transponder hardware distortions. In annex B, simulated end-to-end BER performance and spectral characteristics of most of the recommended modulations are provided for a selected channel model (the SSPA reference model in annex B) and no hardware distortions.

Table 4-1: CCSDS Recommendations on Bandwidth-Efficient Modulations

Frequency Band	Applicable CCSDS Recommendation(s)	Recommended Modulations
2200-2290 MHz 8450-8500 MHz	401 (2.4.17A) B-1	• GMSK BT_s=0.25 with precoding • Filtered OQPSK
2290-2300 MHz 8400-8450 MHz	401 (2.4.17B) B-1	• GMSK BT_s=0.5 with precoding
8025-8400 MHz	401 (2.4.18) B-1	• 4D-8PSK-TCM • GMSK BT_s=0.25 with precoding • Filtered OQPSK
31800-32300 MHz	401 (2.4.20B) B-1	• GMSK BT_s=0.5 with precoding

ANNEX A

GLOSSARY

AM/AM	Amplitude-dependent amplitude distortion
AM/PM	Amplitude-dependent phase distortion
AGC	Automatic Gain Control
BER	Bit Error Rate
BPSK	Binary Phase Shift Keying
Category A mission	Missions whose altitude above Earth is less than 2×10^6 km
Category B mission	Missions whose altitude above Earth is greater than 2×10^6 km
CCSDS	Consultative Committee on Space Data Systems
CPM	Continuous Phase Modulation
dB	Decibel
E_b/N_o	Energy per bit to Noise spectral density ratio
E_s/N_o	Energy per symbol to Noise spectral density ratio
EESS	Earth Exploration Satellite Service
FSK	Frequency Shift Keying
GHz	Gigahertz
GMSK	Gaussian Minimum Shift Keying
I&D	Integrate-and-Dump
ISI	Inter-Symbol Interference
ITU	International Telecommunication Union
LPF	Low Pass Filter
Ms/s	Mega Symbols Per Second
NRZ	Non-Return to Zero

OBO	Output Back-off
OQPSK	Offset Quadrature Phase Shift Keying
OQPSK I/Q	I/Q Modulated Offset Quadrature Phase Shift Keying
OQPSK/PM	Phase Modulated Offset Quadrature Phase Shift Keying
OSC	Oscillator
PM	Phase Modulated
PSD	Power Spectral Density
R_s	Coded symbol rate at input to modulator
R_b	Information bit rate
R_{ChS}	Channel symbol rate
RF	Radio Frequency
SFCG	Space Frequency Coordination Group
SRRC	Square Root Raised Cosine
SRS	Space Research Service
SSPA	Solid State Power Amplifier
T_s	Coded symbol period at input to modulator
T_b	Bit period
T_{ChS}	Channel symbol period
TCM	Trellis Coded Modulation
TWTA	Traveling Wave Tube Amplifier
VCO	Voltage Controlled Oscillator

ANNEX B

SIMULATED MODULATION PERFORMANCE
WITH SSPA OPERATING IN SATURATION

This annex provides simulated performance data of the efficient modulations described in this Green Book when amplified by an SSPA operating at 0 dB output backoff referenced to maximum output power (corresponding to Input Backoff at –3 dB for the reference SSPA in this annex). This data includes occupied bandwidth, BER with matched filter and I&D receivers, and interference susceptibility. The reader should be aware that the performance of these modulations is highly dependent on the actual receiver and transmitter hardware characteristics including but not limited to the power amplifier linearity and operating point, symbol asymmetry, data imbalance, modulator gain/phase imbalance, local oscillator phase noise and, for digital applications, time/amplitude quantization. **The data provided in this annex is indicative of system performance expected using the reference model. Actual performance is highly dependent upon transmitter and receiver characteristics.**

Only distortions caused by amplifier AM/AM and AM/PM are considered in the results presented in this annex. The AM/AM and AM/PM curves used in the simulations originated from measurements of a 10W SSPA provided by ESA and are shown in figures B-1 and B-2, respectively. The performance data in this annex has been extracted from study reports which can be found in the CCSDS Yellow Book, *Proceedings of the Bandwidth-Efficient Modulations Working Documents* (reference [1]).
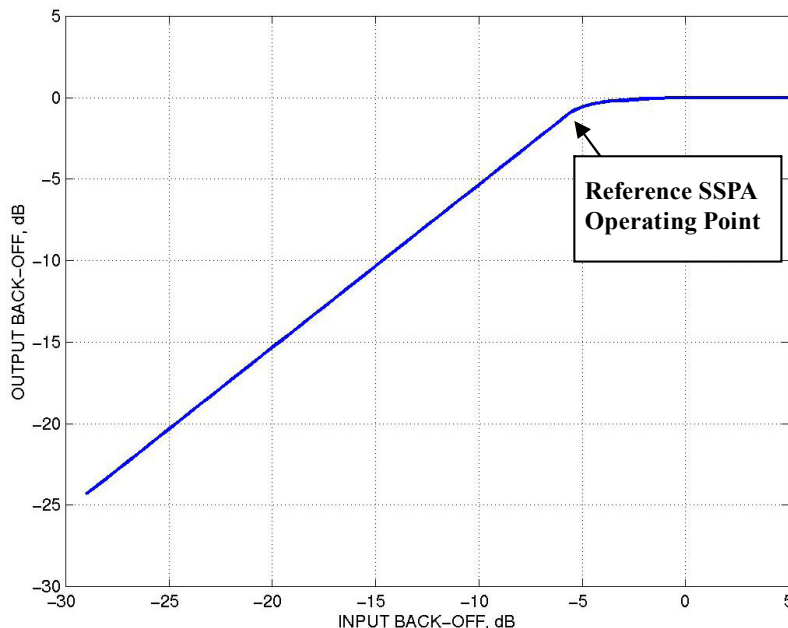
Figure B-1: AM/AM Characteristic of Reference SSPA
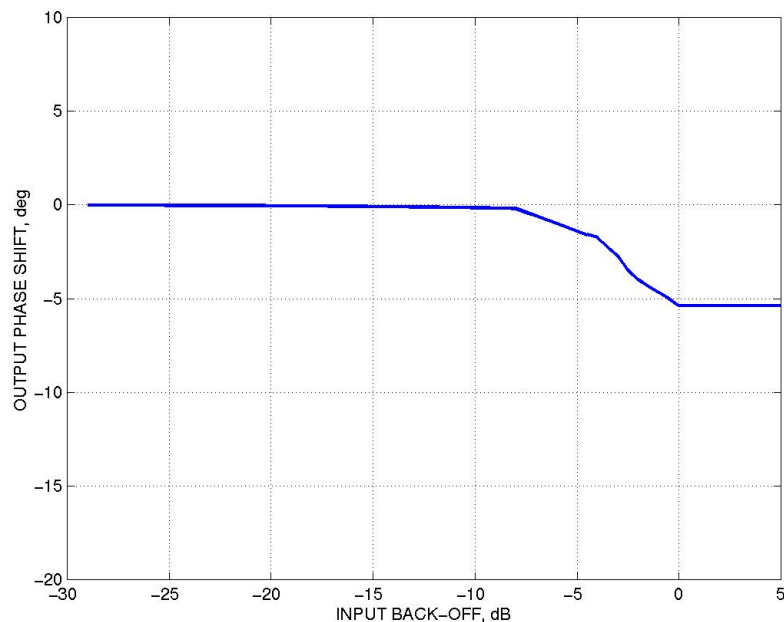
Figure B-2: AM/PM Characteristic of Reference SSPA

B1   OCCUPIED BANDWIDTH

In the CCSDS studies on bandwidth-efficient modulations (reference [1]) which provided the data for this subsection, the user spacecraft power amplifier was assumed to be operated at 0 dB OBO reference point. This mode of operation allows for the most efficient use of limited spacecraft onboard power and is consistent with the vast majority of Category B missions as well as many Category A missions. A side effect of operating near saturation is that the amplifier will introduce to a non-constant envelope signal nonlinear distortions which can result in the regeneration of filtered sidelobes. This effect is known as spectral regrowth. In this subsection, the spectral containment of the recommended modulations after a saturated power amplifier as measured by the occupied bandwidth is detailed.

Occupied bandwidth is defined by article 1.153 of the ITU Radio Regulations (ITU RR) as *the width of a frequency band such that, below and above the upper frequency limits, the mean powers emitted are each equal to a specified percentage β/2 of the total mean power of a given emission*, where β is taken to be 1%. For β = 1%, this is often referred to as the 99% power containment bandwidth.

Table B-1 shows the simulated occupied bandwidths normalized to the symbol rate[7] at the input to the modulator of selected bandwidth-efficient modulations recommended for Category A space-to-Earth links at the output of a saturated SSPA. In addition, the normalized –60 dB bandwidths[8] are given. Table B-2 shows the occupied bandwidths for Category B recommended efficient modulations.

Table B-1:   Occupied Bandwidth of Category A Recommended Efficient Modulations after Spectral Regrowth Due to Saturated SSPA

Modulation Type	Two Sided -60 dB Bandwidth [9]	Occupied Bandwidth
Unfiltered BPSK [9]	635 R_s	20.56 R_s
Baseband Filtered OQPSK/PM		
Butterworth 6th order BT_s=0.5	2.70 R_s	0.88 R_s
SRRC (α=0.5)	2.68 R_s	0.88 R_s
Bessel 6th order BT_s=0.5	3.69 R_s	0.93 R_s
Baseband Filtered OQPSK I/Q		
Butterworth 6th order BT_s=0.5	4.06 R_s	0.86 R_s
SRRC α=0.5	4.24 R_s	0.88 R_s
Bessel 6th order BT_s=0.5	4.95 R_s	1.34 R_s
Precoded GMSK BT_s = 0.25	2.14 R_s	0.86 R_s

Table B-2:   Occupied Bandwidth of Category B Recommended Efficient Modulations after Spectral Regrowth Due to Saturated SSPA

Modulation Type	-60 dB Bandwidth	Occupied Bandwidth
Precoded GMSK BT_s=0.5	3.02 R_s	1.03 R_s

B2   SIMULATED END-TO-END BER PERFORMANCES

B2.1   UNCODED BIT ERROR RATE (BER) PERFORMANCE IN A NON-LINEAR CHANNEL

As a general matter, all of the bandwidth-efficient modulation techniques included in these recommendations provide acceptable BER performance for use in space data systems. However, for each of these modulations, the precise BER performance of any given system is dependent upon the detection algorithm used in the receiver. Accordingly, a meaningful characterization of the BER performance of each modulation type must include some insight into the performance of the modulation type with the receiver types likely to be used.

---

[7] See 2.4 for bit/symbol terminology definitions used in this Green Book.

[8] The –60 dB bandwidth is defined here as the frequency band such that, below the lower frequency limit and above the upper frequency limit, the continuous power spectral density does not exceed –60 dB/Hz below the peak PSD over any 1 Hz bandwidth. This level is chosen to coincide with the floor of the SFCG 21-2 spectral emissions mask.

[9] For reference purposes only; not part of bandwidth-efficient modulation recommendation.

The optimal receivers needed to achieve the theoretical BER performance for these modulation types incorporate precisely matched filters and, in some cases, the use of a Viterbi detection algorithm. In many cases, nearly optimal performance can be achieved using a considerably simpler and less costly receiver structure. The uncoded performance of some bandwidth-efficient modulations, including those recommended by the CCSDS, using the receiver types deemed most likely to be employed are summarized in table B-3 below.

Table B-3: **Simulated Uncoded BER Performance of Recommended Category A Efficient Modulations with Distortions Due to Saturated SSPA**

Modulation Type	Receiver Type	E_b/N_o for 10^{-3} BER	E_b/N_o for 10^{-5} BER	CCSDS Yellow Book Reference
Unfiltered BPSK (for reference only)	Integrate and Dump	6.8 dB	9.6 dB	Sections 1-05, 1-12

Baseband Filtered OQPSK/PM
    Butterworth 6th order BT_s=0.5
    SRRC α=0.5
    Bessel 6th order BT_s=0.5
	Integrate and Dump	7.6 dB
		7.6 dB
		7.6 dB
			10.5 dB
			10.6 dB
			10.8 dB
				Section 1-07

Baseband Filtered OQPSK I/Q
    Butterworth 3rd order BT_s=0.5
    Butterworth 6th order BT_s=0.5
    SRRC α=0.5
    Bessel 6th order BT_s=0.5
	Integrate and Dump	7.4 dB
		7.4 dB
		7.4 dB
		7.4 dB
			10.5 dB
			10.5 dB
			10.5 dB
			10.5 dB
				Section 1-07

Pulse-Shaped SRRC α=0.5	Matched Filter	7.4 dB	10.5 dB	Sections 1-05, 1-12
Precoded GMSK BT_s=0.25	Viterbi Receiver	7.0 dB	10.0 dB	Sections 1-05, 1-12

Table B-4: **Simulated Uncoded BER Performance of Recommended Category B Efficient Modulations with Distortions Due to Saturated SSPA**

Modulation Type	Receiver Type	E_b/N_o for 10^{-3} BER	E_b/N_o for 10^{-5} BER	CCSDS Yellow Book Reference
Precoded GMSK BT_s=0.5	Viterbi Receiver	6.8 dB	9.7 dB	Sections 1-05, 1-12

B2.2 CODED BIT ERROR RATE (BER) PERFORMANCE IN NON-LINEAR CHANNEL

Forward error correcting codes can be used to reduce the E_b/N_o required to meet BER requirements. This subsection provides simulated BER of selected bandwidth-efficient modulations using the CCSDS standard rate ½, k=7 convolutional inner code concatenated with a (255,223) Reed-Solomon outer code. The BER simulations included a model of a 10W ESA SSPA whose AM/AM and AM/PM characteristics are shown in figures B-1 and

B-2, respectively. The Viterbi decoder in the simulations used 3-bit quantization of the metrics and a decoding depth of 70 bits. In the simulations, a Reed-Solomon interleaving depth of 5 was used. A coding gain on the order of 0.1 dB can be obtained by using 8-bit quantization instead of 3-bit quantization.

Table B-5: Simulated BER Performance of Category A Efficient Modulations with Concatenated Code in Non-Linear Channel

Modulation Type	Receiver Type	E_b/N_o for 10^{-6} BER	CCSDS Yellow Book Reference
Unfiltered BPSK (reference only)	Integrate and Dump	2.55 dB	Sections 1-06, 1-14

Baseband Filtered OQPSK/PM
    Butterworth 6th Order BT_s=0.5
    SRRC α=0.5
	Integrate and Dump	3.09 dB
		3.16 dB
			N/A

Baseband Filtered OQPSK I/Q
    Butterworth 3rd order BT_s=0.5
    Butterworth 6th order BT_s=0.5
    SRRC α=0.5
	Integrate and Dump	2.91 dB
		3.04 dB
		3.06 dB
			Sections 1-06, 1-14

Pulse-Shaped SRRC α=0.5	Matched Filter	2.77 dB	
Precoded GMSK BTs=0.25	Quasi-Matched Filter + 3 tap equalizer	2.73 dB	Sections 1-06, 1-14

Table B-6: Simulated Uncoded BER Performance of Recommended Category B Efficient Modulation with Concatenated Code in Non-Linear Channel

Modulation Type	Receiver Type	E_b/N_o for 10^{-6} BER	CCSDS Yellow Book Reference
Precoded GMSK BT_s=0.5	Quasi-Matched Filter	2.58 dB	Sections 1-06, 1-14

B2.3   4D-8PSK-TCM BER PERFORMANCE

Figure B-4 shows the simulated bit error performance of 4D-8PSK-TCM with 2, 2.25, 2.5 and 2.75 bits/channel-symbol efficiencies. The simulation results were obtained under the assumptions of a linear communications chain (i.e., linear power amplifier and linear 8PSK modulator in AWGN channel). As such, these results should not be compared with the BER results from B2.1 and B2.2 which assume non-linear power amplification.

The TCM decoder used for simulations is based on the implementation of the Viterbi algorithm (see figure B-3) but simplified with the 'trace-back' method (reference [10]), which consists of choosing the survivor from the first node of the trellis only, assuming a sufficient truncation length. The number of parallel information bits m obtained before coding is 8, 9, 10 or, 11 bits, according to the channel efficiency. The branch metrics (BM) are coded with 4 bits while cumulated metrics in 'Add Compare and Select' (ACS) operator are coded with 5 bits. The Viterbi algorithm is applied to a 64 states decoder with 8 branches per state and a truncation path length equal to 36. The output delivers m bits at a time which corresponds to the decoded information after processing of four successive phase states.
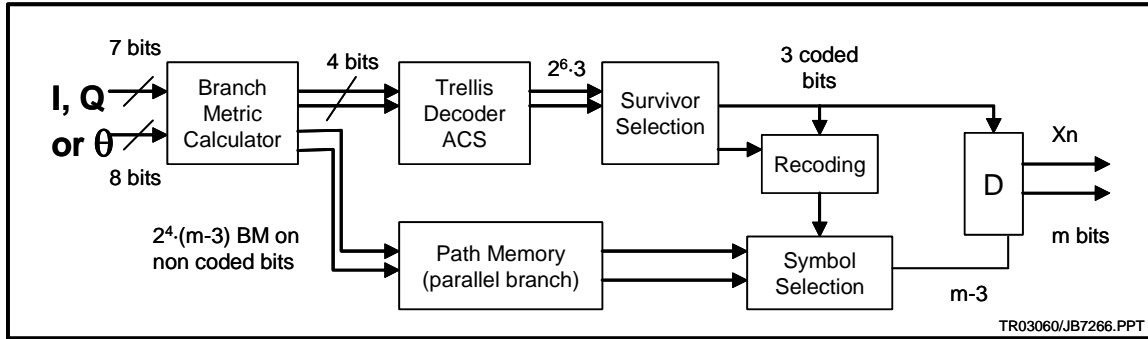
Figure B-3: Principle of the 4D-8PSK-TCM Decoder Used in Simulations

The BER obtained with the simulations is given in figure B-4 for the four efficiencies (plain curves). The dotted curves correspond to the lower bound (asymptotic curves) obtained from calculations taking into account the different minimum Euclidian distances obtained for each efficiency. Theoretical uncoded QPSK and 8PSK BER are given as reference.

BER performance comparison
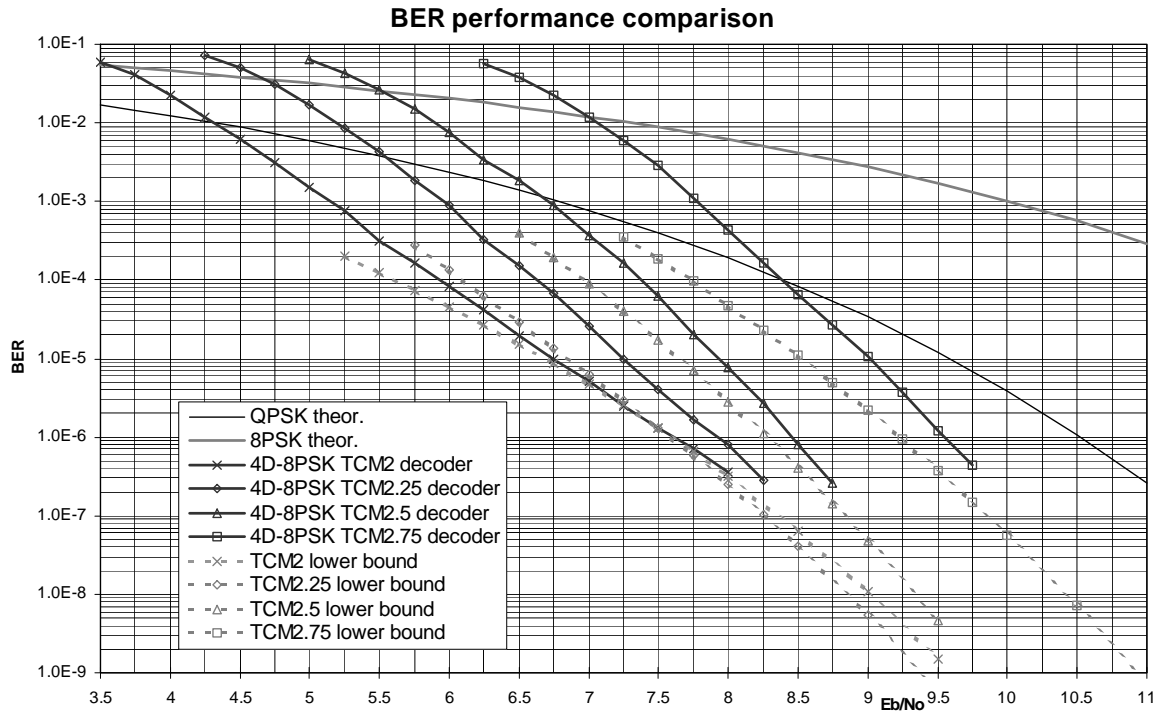
Figure B-4: 4D-8PSK-TCM BER vs. E_b/N_o in dB for 2, 2.25, 2.5, and 2.75 Bits/Channel Symbols

B3 END-TO-END PERFORMANCES – INTERFERENCE SUSCEPTIBILITY

Interference susceptibility is defined as the degradation in E_b/N_o to the victim modulation caused by an interfering signal source operating in the same or adjacent allocated frequency band. To a first order, interference susceptibility of a modulation is determined by the characteristics of the receiver detection filter. Thus the recommended bandwidth-efficient modulations with matched filter receivers are in general more susceptible to narrowband interference close to the carrier frequency than unfiltered BPSK but less susceptible to interference away from the carrier frequency because of the frequency response of the matched filter. This also holds true for wideband interference, although to a lesser extent as the interference is spread over a wider frequency range. In the limit as the interference becomes so wideband that it looks like white noise, the recommended modulations are roughly equally susceptible.

Likewise, if the same detection filter is used to detect all modulations (e.g., an integrate-and-dump filter), the interference susceptibility of the modulations is also roughly equivalent (reference [5]). Second order effects that affect interference susceptibility include the relative phase of the interferer with respect to the victim signal, the receiver Automatic Gain Control (AGC) and the carrier tracking loop.

B3.1   NARROWBAND INTERFERENCE

Table B-7 shows simulation results (reference [11]) on the minimum frequency separation between a narrowband interferer and the efficient modulation before the victim modulation suffered a specified E_b/N_o loss. The smaller the minimum interference frequency offset, the less susceptible the modulation is to narrowband interference. As the table shows, the more bandwidth efficient the modulation, the closer the interfering tone could be before a 1 dB degradation occurred.

In these simulations, the narrowband interferer was modeled as a tone with equal power as the victim. The channel model consists of the reference SSPA operating at 0 dB output backoff with respect to maximum output power. The loss is measured with respect to the E_b/N_o required for each modulation to achieve 10^{-3} uncoded BER (including the effects of the SSPA) when there was no interference. Thus the degradation in the tables is the loss solely due to the interference and excludes any inherent modulation loss. Matched filters or quasi-matched filters were used in the simulations.

Table B-7: Narrowband Interference Susceptibility

Modulation Type	Minimum Interference Offset from f_c for Specified E_b/N_o Loss			
	0.25 dB Loss	0.50 dB Loss	0.75 dB Loss	1.00 dB Loss
Unfiltered BPSK	2.5 R_s	1.7 R_s	1.6 Rs	1.5 R_s
Filtered OQPSK[10]	0.7 R_s	0.47 R_s	0.45 R_s	0.43 R_s
SRRC-OQPSK	0.38 R_s	0.37 R_s	0.36 R_s	0.35 R_s
Precoded GMSK BT_s=0.5	0.6 R_s	0.58 R_s	0.53 R_s	0.5 R_s
Precoded GMSK BT_s=0.25	0.52 R_s	0.49 R_s	0.47 R_s	0.46 R_s

B3.2   WIDEBAND INTERFERENCE

When bandwidth-efficient modulations are first deployed, a likely source of wideband interference will be legacy BPSK systems overlapping into the victim's frequency allocation. Table B-8 shows the wideband interference susceptibility (reference [11]) of selected CCSDS-recommended bandwidth-efficient modulations with the wideband interference modeled as an unfiltered BPSK signal with equal power and data rate but with random phase offset to the victim modulation. The smaller the interference frequency offset, the less susceptible to interference the modulation is. The simulated channel model consisted of a SSPA operating at 0 dB output backoff referenced to maximum output power. As in table B-7, loss is measured with respect to the E_b/N_o required for 10^{-3} BER with no interference (i.e., loss due to interference only).

---

[10] Third order baseband Butterworth filter with BT_s = 0.5.

Table B-8: Wideband Interference Susceptibility

Modulation Type	Minimum Interference Offset from f_c for Specified E_b/N_o Loss			
	0.25 dB Loss	0.50 dB Loss	0.75 dB Loss	1.00 dB Loss
Unfiltered BPSK	> 3 R_s	2.5 R_s	2.4 R_s	1.8 R_s
Filtered OQPSK[10]	1.05 R_s	0.96 R_s	0.88 R_s	0.8 R_s
SRRC-OQPSK	1.3 R_s	1.0 R_s	0.93 R_s	0.9 R_s
Precoded GMSK BT_s=0.5	1.3 R_s	1.18 R_s	1.12 R_s	1.09 R_s
Precoded GMSK BT_s=0.25	1.06 R_s	0.98 R_s	0.90 R_s	0.85 R_s

B3.3   CO-CHANNEL INTERFERENCE

Table B-9 shows the interference susceptibility of the recommended modulations assuming that the interferer is of the same modulation type as the victim (reference [12]). Here, the interference susceptibility is measured by the required victim-power-to-interferer-power ratio, P_s/P_I, that caused a degradation of 1 dB with respect to ideal BPSK in AWGN at BER equal to 10^{-1}, 10^{-2}, and 10^{-3}. The higher the value of P_s/P_I, the more susceptible to interference the modulation is. Table B-9 shows the values for P_s/P_I with the co-channel interferer centered at the victim carrier frequency, and at a frequency offset a quarter times the coded symbol rate at the input to the modulator. The simulated channel model consisted of the reference SSPA operating at 0 dB output backoff with respect to maximum output power. In the results in table B-9, the interferer is assumed to have a worst-case phase and timing offset that causes the largest amount of degradation.

Table B-9: Co-Channel Interference

Interference Frequency Offset	Modulation Type	P_s/P_I for BER=10^{-1}	P_s/P_I for BER=10^{-2}	P_s/P_I for BER=10^{-3}
0	Unfiltered BPSK	9.21 dB	13.69 dB	15.45 dB
	Filtered OQPSK[10]	9.69 dB	15.50 dB	18.81 dB
	SRRC OQPSK	9.39 dB	15.71 dB	19.84 dB
	Precoded GMSK BT_s = 0.5	7.40 dB	12.24 dB	14.39 dB
1/(4T_s)	Unfiltered BPSK	5.20 dB	10.06 dB	12.19 dB
	Filtered OQPSK[10]	7.63 dB	13.39 dB	16.69 dB
	SRRC OQPSK	7.32 dB	13.63 dB	17.78 dB
	Precoded GMSK BT_s = 0.5	5.55 dB	10.80 dB	13.21 dB

B4 CROSS-SUPPORT BER PERFORMANCE

B4.1 INTEGRATE AND DUMP RECEIVER

Cross support is defined here as the ability for a modulation to be successfully demodulated and detected by a receiver designed for a different modulation. The modulations recommended in recommendations 401 (2.4.17A) B-1, 401 (2.4.17B) B-1, and 401 (2.4.20B) B-1 can all be viewed as OQPSK-type modulations. Thus it is not surprising that in many cases a matched filter receiver designed for a particular recommended OQPSK-type modulation is able to cross-support other recommended OQPSK-type modulations, although with some E_b/N_o degradation due to filter mismatch. However, this is true only for receivers with symbol-by-symbol detection; receivers based on trellis demodulation in general will not be compatible with other modulations unless the trellis codes are compatible. Also, 4D-8PSK-TCM in recommendation 401 (2.4.18) cannot be cross-supported by an OQPSK-type receiver without substantial receiver modifications.

Of particular interest in terms of cross support is the integrate-and-dump-type receiver that is present in many ground stations at the present time. Table B-10 shows the simulated uncoded E_b/N_o degradation of some recommended Category A bandwidth-efficient modulations using an I&D receiver and assuming the reference SSPA model operating at 0 dB output backoff with respect to maximum output power. Table B-11 shows the same data except for uncoded Category B recommended efficient modulations. The loss in tables B-10 and B-11 is measured with respect to ideal BPSK.

Table B-10: Simulated Uncoded Loss of Category A Efficient Modulations Using I&D Receiver

Modulation Type	Loss at BER = 10^{-3}	Loss at BER = 10^{-5}
Baseband Filtered OQPSK/PM		
Butterworth 6th order BT_s=0.5	0.8 dB	1.1 dB
SRRC α=0.5	0.8 dB	1.4 dB
Bessel 6th order BT_s=0.5	0.5 dB	0.8 dB
Baseband Filtered OQPSK I/Q		
Butterworth 3rd order BT_s=0.5	0.6 dB	0.9 dB
Butterworth 6th order BT_s=0.5	0.6 dB	0.9 dB
Pulse-Shaped SRRC α=0.5	1.1 dB	1.7 dB
SRRC α=0.5	0.6 dB	0.9 dB
Bessel 6th order BT_s=0.5	0.6 dB	0.9 dB
Precoded GMSK BT_s = 0.25	1.2 dB	1.7 dB

Table B-11: Simulated Uncoded Loss of Recommended Category B Efficient Modulations with I&D Receiver

Modulation Type	Loss at BER = 10^{-3}	Loss at BER = 10^{-5}
Precoded GMSK BT_s = 0.5	0.8 dB	1.2 dB

B4.2   OTHER RECEIVERS

Table B-12 shows the simulated uncoded Eb/No required for 10^{-3} BER of some recommended bandwidth-efficient modulations using different types of receivers assuming the reference SSPA model operating at 0 dB output backoff with respect to maximum output power.

Table B-12: Cross Support BER Performance of Recommended Modulation Formats Using Other Receiver Types

Receiver Type	Transmitter Type	
	GMSK	Filtered OQPSK
GMSK	7.1 dB	7.1 dB
Filtered OQPSK	7.5 dB	7.3 dB
OQPSK	8.0 dB	7.4 dB